skb.se

SKB R-24-13

ISSN 1402-3091
ID 2053022
December 2025

Modelling CFC concentrations in MIKE SHE - attempting to recreate estimated groundwater age distributions using limited concentration data

Elin Jutebring Sterte
DHI

Keywords: Chlorofluorocarbon, CFC, MIKE SHE, Hydrology, Tracer

Abstract

This study examines a hydrological model of the Krycklan catchment in MIKE SHE wherein groundwater Chlorofluorocarbon (CFC) concentration data is used to aid in model calibration in order to assess the validity of modelled groundwater transport times. Limited spatial and temporal resolution of the CFC result in a large modelled uncertainty surrounding groundwater transport times; insufficient groundwater data at depths greater than 2 m results in significant uncertainty pertaining to whether CFC concentrations at these depths have reached maximum concentrations. Results of this study do however highlight the capability of using CFC concentration data as a means to aid in the calibration of porosity.

Sammanfattning

Denna studie undersöker en hydrologisk modell av Krycklan avrinningsområde i MIKE SHE, där grundvattenkoncentrationer av klorfluorkarboner (CFC) används för att hjälpa till med kalibreringen av modellen i syfte att bedöma giltigheten av de modellerade transporttiderna i grundvattnet. Begränsad upplösning av CFC koncentrationsdata i både tid och rum CFC-data resulterar i stor osäkerhet i de modellerade transporttiderna för grundvatten; otillräckliga koncentrationsdata på djup större än 2 m leder till betydande osäkerhet kring huruvida koncentrationerna av CFC på dessa djup har nått sina maximala nivåer. Resultaten från denna studie visar dock på potentialen att använda uppmätta CFC-koncentrationer som ett verktyg för att kalibrera porositet.

Content

1 Introduction

Management of radioactive waste and spent nuclear fuel in Sweden is the responsibility of the Swedish Nuclear Fuel and Waste Management Company (SKB). The deposition of radioactive waste and spent nuclear fuel in designated final repositories is a key step in the waste management chain. As a part of the licencing applications for these final repositories, the long-term radiological safety of each repository is continually assessed wherein hydrological and hydrogeological modelling are key components of the safety assessments.

Site descriptive modelling of the hydrology at Forsmark as presented in Bosson et al. (2008) has provided the basis on which predictive, future hydrological models for Forsmark were built (Bosson et al., 2010, Werner et al., 2013). A large amount of measured time-series and point data are used to calibrate and validate the site descriptive hydrological model (see Chapter 2 in Bosson et al. (2008). A large amount of hydrological data was used to calibrate and validate the site-descriptive hydrological model presented in Bosson et al. (2008) was not used. However, hydrological tracer data, which can reveal groundwater travel and residence times, was excluded from the calibration and validation process.

This report investigates the potential to include measurements of Chlorofluorocarbons (CFCs) in groundwater in the calibration steps of the hydrological site-descriptive modelling. While this study focuses on CFC data gathered with the Krycklan catchment and uses a MIKE SHE hydrological model produced for that same catchment to evaluate the CFC data, results are intended to inform on the potential of using CFC data to aid in the evaluation of the site-descriptive hydrological modelling at Forsmark.

1.1 Background

Travel times, defined as the time from groundwater recharge to a certain point, gives fundamental information regarding a catchment's hydrological and biogeochemical processes (McDonnell, et al., 2010; Sprenger, et al., 2018). This includes, but is not limited to, transport and dispersal of contaminants, accumulation of organic carbon and weathering rates (Burns, et al., 2003; Kralik, 2015). Even if the main proportion of water discharging in streams is relatively young (less than three months), there is often a portion that can span ages from years to decades (Jasechko, et al., 2017; von Freyberg, et al., 2018; Stockinger, et al., 2019). Research has shown that travel times tend to rapidly increase with flow path length as well as soil depth, but to what extent is still uncertain (Cardenas, 2007).

Biogeochemical tracers and stable isotopes are common tools to investigate water flow paths and travel times (Kazemi, et al., 2006). Isotopic time-series analysis can be used to quantify travel times (Tetzlaff & Soulsby, 2008; Karlsen, et al., 2016). Mean travel times can also be estimated using isotopic tracer signal-dampening (Peralta-Tapia, et al., 2015). The main advantage of isotopes is that they are relatively conservative, while other tracers can transform due to chemical reactions along the travel path (Goller, et al., 2005). However, there have been shown to be difficulties assessing ages longer than five years when using isotopes due to amplitude loss during the mixing of young and old groundwater (Kirchner, 2016). However, isotopes can still be used to assess the young water fraction.

In Jutebring Sterte et al. 2021a base cations concentrations and isotopic signals, in combination with particle tracking in a MIKE SHE 3D model, were used to investigate and showcase the variation in proportion of old and young water fractions. The study was focused on the young water fraction (water less than three months old) as well as travel times of groundwater contributions to streams across a catchment. The model study was based on Krycklan, and a strong correlation between isotopic signal change from winter to spring was found, which correlated well with modelled young water fractions. Streams with high base cation concentrations due to longer weathering time were also associated with longer modelled travel times. The study showed that it's possible to represent flows and groundwater levels with a MIKE SHE model and capture important space and time-varying functions, important for many different biogeochemical processes.

Other tracers that can be used to assess groundwater travel times are the atmospheric tracers' chlorofluorocarbons (CFCs) (Chambers, et al., 2019). CFCs were widely used in, e.g. refrigerators and air conditioning starting in the 1930s-40s, increasing the CFC concentration exponentially in the atmosphere (Kim, et al., 2011; Chambers, et al., 2019). CFCs has been found to impact the stratosphere by depleting the ozone layer. This led to the Montreal Protocol in the late 1980s, which resulted in a drastic decrease in the use of CFCs. As a result, CFC concentrations levelled off and decreased in the 1990s. Due to their usage history being relatively well accounted for, CFCs have been used to date water up to 50 years old (Cook & Solomon, 1997; Chambers, et al., 2019; Darling, et al., 2012). It is generally assumed that the tracers' concentrations are at equilibrium with the atmosphere when recharged to the saturated zone. CFCs (including CFC-11, CFC-12 and CFC-113) are relatively conservative, although sorption, contamination or degradation may occur (Plummer and Busenberg, 2000). They are also considered ideal tracers according to Henry's Law since they become dissolved in groundwater and have been released at known rates worldwide over many decades. Moreover, CFC-12 is less reactive than CFC-11 and CFC-113 in anoxic conditions. It could then be argued that CFC-12 would most likely be a better representation of groundwater ages than the other two CFCs (Kolbe, et al., 2020). Due to the nature of CFC-12, it could potentially be used to track groundwater for about 50-years.

1.2 Study objectives

This study aims to: 1.) Update the Krycklan model with new data (2009-2022), 2.) Fine-tune model calibration using additional streamflow and groundwater data, and 3.) Calibrate the model with CFC data to assess travel times.

The main objective of this study is to evaluate the potential of using CFC-12 to enhance the accuracy of soil property calibration in MIKE SHE for groundwater travel time estimation.

1.3 Study setting: Krycklan

The Krycklan catchment is located in northern Sweden (see Figure1-1) in the temperate/subarctic climate zone (N 7131677 E 731035.8 SWEREFF99 TM), where the topography varies between 114 and 405 m.a.s.l (Laudon, et al., 2021). This region is usually covered by snow during six months of the year, has an average temperature of 1.8˚C, an annual precipitation of 614 mm and a mean annual runoff of 311 mm (Laudon, et al., 2013).

Above the highest postglacial coastline to the northwest of the Krycklan catchment, the soils consist mainly of glacial tills reaching depths up to approximately 20 m. A few lakes and peatlands are also located within this area. The deeper soils consist of a basal till compacted by moving ice from the last glacial period. Shallower soils consist primarily of ablation till. A decreasing hydraulic conductivity with depth is characteristic for glacial till in northern Sweden (Bishop, et al., 2011; Nyberg, 1995). Below the highest postglacial coastline, to the southeast, soils primarily consist of glaciofluvial deposits of primarily sandy and silty sediments. Here, the soil depth is much deeper, reaching at least 50 m in some places.

Streamflow is monitored for 14 nested sub-catchments, called C1 to C20. This study will focus on the C9 sub-catchment, which includes C2, C4, C5, C6, and C7.

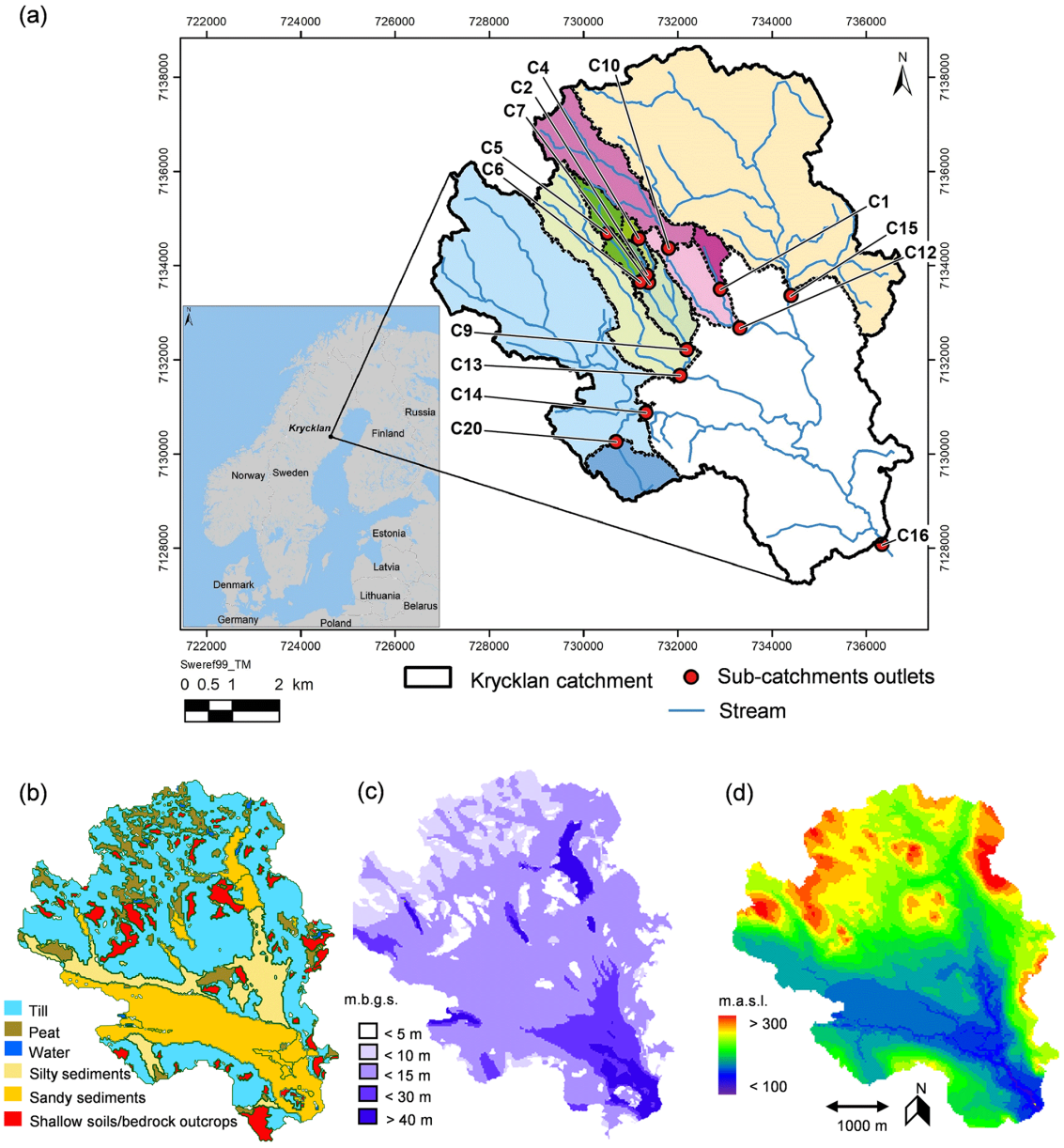

Figure 1-1. *The Krycklan catchment (Jutebring Sterte, et al., 2021a). The figure showcases the locations of sub-catchments and their outlet stream monitoring stations (a), the soil property map, (b), the depth to bedrock map in meters below the ground surface (m.b.f.s.) (Swedish Geological Survey (SGU), 2016) (c) and the catchment elevation in meter above sea level (m.a.s.l.) (d).*

2 Method

2.1 General model setup and model tool

In this study we applied MIKE SHE coupled to MIKE 11 (Figure 2-1). These are hydrological modelling tools used to simulate the hydrological system for catchments in a 3D setting and are provided by Mike Powered by DHI (DHI, 2023). MIKE SHE is a hydrogeological model that calculates flow fluxes from different compartments and model cells at each model time step and can be run in both steady state and transient conditions (Graham & & Butts, 2005). MIKE SHE calculates both evapotranspiration and precipitation in both liquid and frozen state (snow). It is also able to simulate flow fluxes between saturated and unsaturated conditions as well as overland flow. In the present study, the overland flow is calculated using 2D diffusive wave approximation of the Saint-Venant equations. A 3D implementation of Darcy's Law and a 1D implementation of Richards's equation were used in this model for saturated and unsaturated conditions, respectively (source). For saturated conditions, a 3D implementation of Darcy's equations is used. For unsaturated conditions, a 1D implementation of Richards's equation is used. For each time step, MIKE SHE is coupled with MIKE 11, which handles surface flow using a high-order dynamic wave formulation of the Saint- Venant equations. The stream model is not restricted to the resolution of the MIKE SHE model and allows for more precise stream flow calculations.

The current MIKE SHE model is based on the model setup presented in table 2.1. It spans the period from 2009 to the end of 2014 (with a few months run-up period in 2008) and was calibrated using flow and groundwater observations. In the current version, new data for precipitation, potential evapotranspiration, flow, and groundwater measurements have been acquired, allowing the model to be extended to 2022-10-01. The pre-existing set-up was used as the initial conditions. However, using the newly acquired data the MIKE SHE model calibration is finetuned in a later stage (section 0).

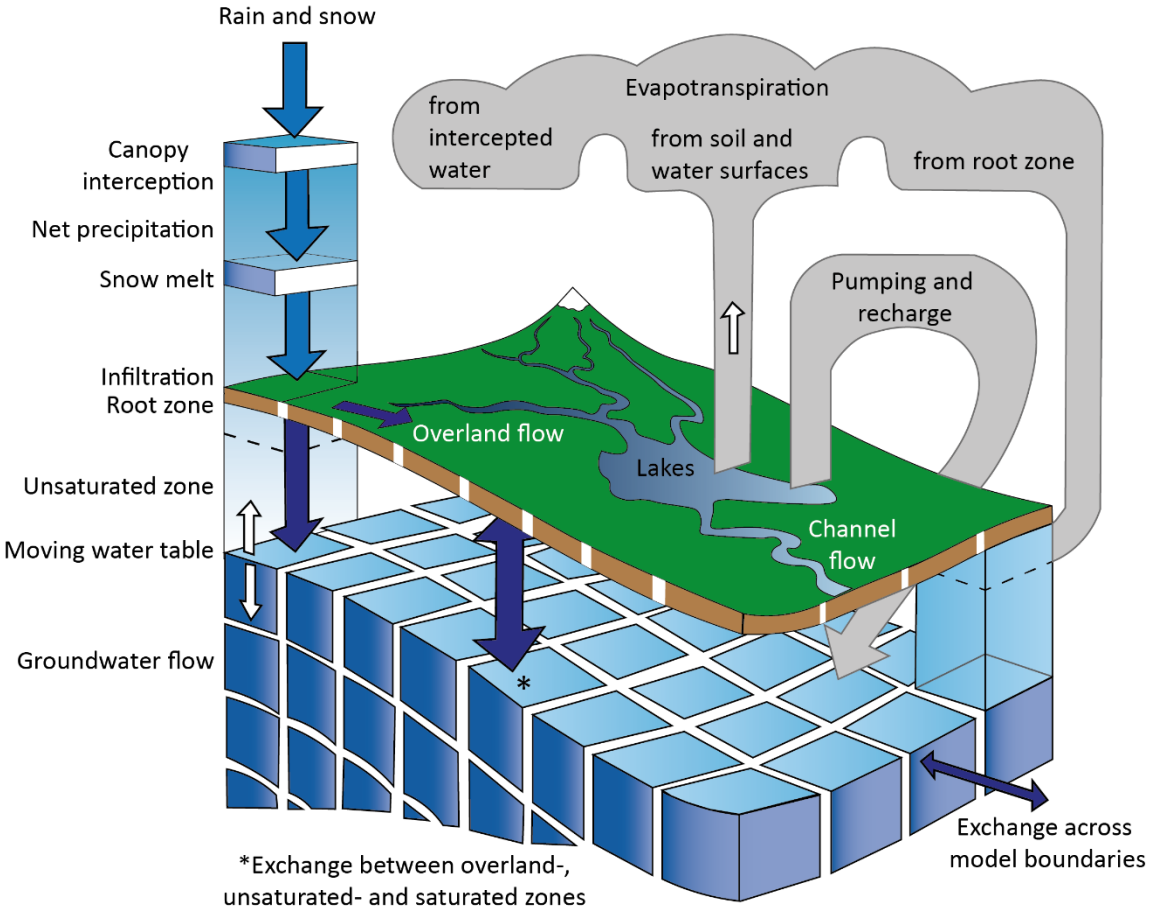

Figure 2-1. *A schematic figure of MIKE SHE and its components (DHI, 2024)*

Climate data to extend the model from 2015 to 2022 originates from the Kyran data service and includes precipitation and temperature (Tejshree, 2023). Data for potential evapotranspiration was modelled and created by Alejandro Scherzis and received from Tamara Kolbe on 23-01-26.

The initial MIKE SHE model set up is based on the models presented in Jutebring Sterte, et al. (2018) and Jutebring Sterte, et al., (2021a). The reader is referred to these publications for in-depth information regarding the model. The MIKE SHE model has a horizontal grid resolution of 50 × 50 m and the lower boundary extends to 100 m below the soil surface. Vertically, the saturated zone is divided into ten calculation layers. The unsaturated zone has finer vertical discretisation ranging from the order of centimetres, when discretizing the model close to the surface, to the order of meters when discretizing the deeper soils of the model. A no-flow boundary condition is applied at the topographical boundaries around the model domain and at the bottom of the model. One exception is for the sand deposit located at the lower elevations of the catchment, where we allow water to flow in and out of the model domain based on groundwater heads measured close to the catchment boundaries. The calibrated soil properties are shown in Table 2-1 and are a part of the calibration to finetune the updated model with newly acquired data (section 2).

Table 2-1 – Model properties, including horizontal and vertical hydraulic conductivities, as well as porosity, for each surface soil type shown in Figure 1-1. The table also showcase the vertical extent of each soil type. This table has been adapted from (Jutebring Sterte, et al., 2021b)

Soil type surface	Depth below ground (m)	Soil type	Horizontal hydraulic conductivity (m/s)	Vertical hydraulic conductivity (m/s)	Porosity
Till	2.5	Till	2×10^{-5}	2×10^{-6}	0.3
	To max soil depth	Fine till	1×10^{-6}	1×10^{-7}	0.3
	Bedrock		1×10^{-9}	1×10^{-9}	0.0001
Peat	5	Peat	1×10^{-5}	5×10^{-5}	0.5
	7	Clay	1×10^{-9}	1×10^{-9}	0.55
	To max soil depth	Fine till	1×10^{-6}	1×10^{-7}	0.3
	Bedrock		1×10^{-9}	1×10^{-9}	0.0001
Silty sediments	3	Silt/clay	1×10^{-7}	1×10^{-7}	0.55
	To max soil depth	Fine till	1×10^{-6}	1×10^{-7}	0.3
	Bedrock		1×10^{-9}	1×10^{-9}	0.0001
Sandy Sediments	4	Silt/Sand	2×10^{-5}	2×10^{-5}	0.45
	0.9×max soil depth	Sand	3×10^{-4}	3×10^{-5}	0.35
	To max soil depth	Fine till	2×10^{-7}	2×10^{-8}	0.3
	Bedrock		1×10^{-9}	1×10^{-9}	0.0001

2.2 Flow model calibration methodology

This section describes the flow model calibration with the primary focus of on the soil hydraulic properties, calibrated against streamflow and groundwater levels.

2.2.1 Calibration data

The calibration data includes streamflow measurements and groundwater level measurements. The streams are monitored using e.g., V-notch weirs or gauged at natural control sections combined with pressure transducers (Karlsen, 2016). Hourly and daily data are recorded during ice-free periods. Sites C2, C4 and C7 are heated, and the flow is logged all year around. Most sites had data up to 2020. Site C7 had data up to 2022, while C9, C12 and C20 only had data up to 2017. Flow data was acquired from Tejshree Tiwari (November-2022). Data for C2, C4 and C7 can also be collected from SITES Data Portal (Svartberget Field Research Station, 2023).

Table 2-2 – Stream monitoring data, including number of observations, data set star and end year and station gauge type. The table also includes if the monitoring station is heated during winter, allowing measurements during ice periods. Location of the monitoring stations can be seen in Figure 1-1.

Flow stations	Number of daily observations	Start year	End year	Gauge type	Heated
C1	2749	2009	2020	90° V-notch weir	No
C2	3770	2009	2020	90° V-notch weir	Yes (since 2011)
C4	4633	2009	2022	90° V-notch weir	Yes (since 2011)
C5	3604	2009	2020	120° V-notch weir	Yes (since 2012)
C6	4495	2009	2022	Culvert	No
C7	4684	2009	2021	90° V-notch weir	Yes (since 1981)
C9	2069	2009	2017	Culvert	No
C10	2938	2009	2019	Culvert	No
C12	1832	2009	2017	Venturi flume	No
C13	3138	2009	2019	Trapezoidal flume	No
C14	1828	2009	2017	Natural section	No
C15	2591	2009	2019	Natural section	No
C16	3084	2009	2022	Natural section	No
C20	2012	2009	2017	Culvert	No

Groundwater data are obtained from the SGU and Snowcat wells. The data from the SGU wells (wells 101-105) was obtained from the SGU open data portal (Sveriges geologiska undersökning (SGU), 2022). The SGU wells have been measured the longest and most frequently (~ twice a month, see number of observations, start and end year for respective well in Table 2-3) within the catchment and are measured with a manual acoustic groundwater sounding device, colloquially known as a "plopper" in English or "Klucklod" in Swedish. Some spontaneous measurements have also been taken for the Snowcat groundwater wells. However, it is unknown by what method these were obtained and to what quality the measurements were taken, although "Klucklod" probably was used. More information about the Snowcat wells can be obtained via Krycklan Safe Deposit (Laudon, 2020)

Table 2-3 – Groundwater monitoring data, including number of observations, data set start and end year and well depth. The table also includes some extra information about the location of the wells.

Well	Number of observations	Start year	End year	Depth below ground (m)	Information
101	362	2009	2022	3.8	Located at C7. Meassured using "klucklod".
103	198	2009	2022	4.7	Located at C7. Meassured using "klucklod".
104	232	2009	2022	3.2	Located at C7. Meassured using "klucklod".
105	170	2009	2022	3.1	Located at C6. Meassured using "klucklod".
301	10	2012	2014	3.8	Fully screened well. Located at Site C2
302	12	2012	2014	2.3	Screened at the bottom 1 m. Located at Site C2
303	12	2012	2014	5.2	Screened at the bottom 1 m. Located at Site C2
304	11	2012	2014	10.7	Screened at the bottom 1 m. Located at Site C2
401	10	2012	2014	3.0	Fully screened well. Located at site C2.
402	12	2012	2014	1.9	Screened at the bottom 1 m. Located at site C2.
403	12	2012	2014	3.9	Screened at the bottom 1 m. Located at site C2.
404	12	2012	2014	10.2	Screened at the bottom 1 m. Located at site C2.
501	7	2012	2014	4.0	Fully screened well. Located at site C9.
601	9	2013	2014	6.0	Fully screened well. Located at site C13.

2.2.2 Calibration and validation targets

The flow model has already been calibrated and validated using surface water and groundwater measurements. However, the previous model spans 2009-2015, while the current model spans 2009-2022. Later on, the source of CFC shall also be placed in the groundwater recharge (section 2.3). A source can be applied in the groundwater recharge in MIKE SHE but can be altered if a cell completely dries out due to the unsaturated zone module taking over. To ensure that the model is numerically stable and that the unsaturated zone does not alter the source concentration the first calculation layer must be deep enough such that the groundwater level is always above the lowest level of the first calculation layer. In the previous setup, the depth of the first calculation layer is 2.5 m to capture the most important interactions between the unsaturated zone, evapotranspiration, and the saturated zone. However, to ensure the above criteria, the lower level of the first calculation layer had to be even deeper at some areas. The model therefore is re-calibrated to ensure that flow and groundwater levels are acceptably represented. For this work, the model is calibrated against data between 2009-2016 and validated on data from 2017-2022.

The model primarily focuses on the stream flow data with the most frequently monitored data (daily data) and longest data series. The stations are also scattered across the Krycklan catchment and give important clues to the catchment's functioning. The objective is to capture the general water balance and flow correlation. The water balance is evaluated using accumulated flow. The accumulated flow is the total modelled flow divided by the total observed flow on days with observations. Generally, an accumulated flow of ±30% is considered acceptable, ±20% is considered as good, and ±10% is considered as well-calibrated water balance. The correlation between modelled and observed values is calculated using the correlation coefficient R (Equation 1) and R^2 and is a statistical measurement of how well the model can predict observed flow (Neupane, et al., 2021). R-values can be between -1 and 1. Here, a value of 1 is a perfect positive correlation, 0 is no correlation, and a value of -1 is a perfect negative correlation. The square of R (R^2) is often used to describe how well a model can predict observations. For this study, a value above 0.5 is considered acceptable, a value above 0.6 is considered good, and a value greater than or equal to 0.7 is considered very good.

$$R = \frac{\sum(X_{i,t}-\overline{X_{i,t}})\times(Y_{i,t}-\overline{Y_{i,t}})}{\sum\sqrt{(X_{i,t}-\overline{X_{i,t}})^2\times(Y_{i,t}-\overline{Y_{i,t}})^2}}, \qquad \text{(Equation 1)}$$

With X being the calculated values and Y being the observed values.

Secondly, the model is calibrated to observed heads of the groundwater wells. The main calibration focus is on the SGU wells, which have the most frequently obtained observations over the longest time. To evaluate the model performance, the mean error (ME) and mean absolute error (MAE) are used (Equations 2 and 3). Overall, more observations are taken at shallower soil depths around the catchment, up to a few meters. This, in combination with uncertainties with soil depth and soil composition, will result in a better understanding of the shallower soil properties while leaving the deeper soils a bit more uncertain. Moreover, as the model grid size is 50×50 m, a difference between the observed and modelled groundwater levels is acceptable since it can be difficult to get an exact match on such a scale for several wells located close to each other.

$$ME = \frac{\sum(Y_{i,t}-X_{i,t})}{n} \quad \text{(Equation 2)}$$

$$MAE = \frac{\sum\left|(Y_{i,t}-X_{i,t})\right|}{n} \quad \text{(Equation 3)}$$

With X being the calculated values and Y being the observed values.

It should be noted that the model does not attempt to examine changes in water characteristics, with respect to the CFC concentrations, as the recharging water moves through the unsaturated zone into the saturated zone; CFC concentrations of the infiltrating water are applied directly to the groundwater surface. While the exact effects on modelling results are unknown, it seems likely that CFC the CFC concentration of the infiltrating water would decrease as it moves through the unsaturated zone to the water table. Therefore, it is the author's opinion that the concentration boundary condition for the CFC concentrations, as applied herein, are likely representative of the "maximum" infiltrating CFC concentration given the estimate(s) of the atmospheric CFC concentrations at Krycklan.

2.3 CFC – calibration methodology

2.3.1 Observed data and CFC model set-up

CFC data from 30 groundwater wells was acquired from Tamara Kolbe and is presented in Kolbe and Bishop, 2024. Samples have been taken from wells across the C9 sub-catchment in Krycklan between 2017 and 2022 (Figure 1-1). Most wells have been sampled once while only some wells have been sampled twice. Three wells, including R505, R507, and a second Audry well, are placed very close to the streams and at only a half-meter depth. Since the current model set-up has a top saturated calculation layer of at least 2.5 m, these wells will most likely not be well represented by the model and are, therefore, not used for CFC calibration. A fourth well, w3, is located on a model cell that, due to the grid resolution, has a mix of till and bedrock properties. Therefore, this well was not used for CFC-calibration. The other 26 wells and their corresponding CFC-12 concentration are listed in Table 2-4.

Table 2-4 – Groundwater wells and their corresponding CFC-12 concentration and number of samples for each well. The table also includes the depth of the calculation layer that the well ends in the current model set-up. The samples were taken between 2017-2022 and are reported in Kolbe, 2024.

Well	Sampling top below-ground	Sampling bottom below-ground	Screen type	Depth of calc.-layer	No of samples	Average CFC-12 (pptv)
a25	0.0	1.64	fully screened	2.5	1	269.3
Audrey S	0.1	1.1	at bottom 1m	2.5	1	378.4
R504	0.0	1.17	fully screened	2.5	1	464.1
SGU2	1.6	2.6	at bottom 1m	2.5	2	413.0
SGU4	2.0	3.0	at bottom 1m	2.5	2	358.3
w11	0.0	2.33	fully screened	2.5	1	413.8
w301	0.0	3.85	fully screened	2.5	1	445.4
w302	1.3	2.3	at bottom 1m	2.5	2	284.0
W40	0.0	2.99	fully screened	2.5	1	324.5
w5	0.0	3.11	fully screened	2.5	1	397.6
w9	0.0	2.4	fully screened	2.5	1	375.5
SGU5	2.3	3.3	at bottom 1m	3.0	1	455.3
w18	0.0	2.17	fully screened	3.0	1	356.1
w201	0.0	3.0	fully screened	3.0	2	405.5
w211	1.0	5.7	screened 1-5 m	3.0	1	462.6
W23	0.0	4.03	fully screened	3.0	1	286.4
W41	0.0	2.62	fully screened	3.0	2	372.0
W43	0.0	2.85	fully screened	3.0	1	385.7
w6	0.0	3.65	fully screened	3.0	1	418.4
w13	0.0	5.76	fully screened	4.0	1	362.0
w303	4.2	5.2	at bottom 1m	5.0	2	336.2
w304	9.3	10.3	at bottom 1m	10	2	155.3
w404	8.2	9.2	at bottom 1m	10	2	31.1
w411	9.0	14.1	screened 9-14 m	15	1	263.8
w412	16.88	17.88	at bottom 1m	15	2	200.0
w213	33	47.6	screened 33-48 m	40	1	85.9

CFC-concentration data for the groundwater recharge was also received by Tamara Kolbe (23-01-26), who obtained the data from Virginie Vergnaud (Université de Rennes). The data shows CFC groundwater recharge concentrations every six months. Using linear interpolation, time series for daily concentrations were obtained (Figure 2-2). Concentrations of CFC in the atmosphere started to increase in the 1930s-40s and reduced after the late 1980s ((Plummer and Busenberg, 2000). The time series is used to calculate the concentration of the groundwater recharge across the catchment. The MIKE SHE model calculates daily changes in concentrations in the saturated zone.

The water movement discretisation controls solute transport in MIKE SHE. Advection-dispersion transport uses the cell-by-cell daily groundwater flow, as well as groundwater head, boundary, drain, and exchange flows from the flow model, and is mathematically described by the advection-dispersion equation (Equation 4).

$$\frac{dc}{dt} = -\frac{dc}{dx}v + \frac{d}{dx}\left(D\frac{d}{dx}\right) + R \qquad \text{(Equation 4)}$$

In equation 4, c is the concentration (g/l), v is groundwater velocity (m/s), D is dispersion (m^2/s), and R is the sum of sources and sinks. Assuming no dispersion, the equation can be simplified to Equation 5:

$$\frac{dc}{dt} = -\frac{dc}{dx}v + R \qquad \text{(Equation 5)}$$

Porosity is the new parameter added to calculate advective transport. The porosity values are used to determine the groundwater velocity (v) by dividing the Darcy velocity on the effective porosity according to Equation 6.

$$v = \frac{q}{\mathrm{q}} \qquad \text{(Equation 6)}$$

In equation 6, v is groundwater velocity, q is the Darcy velocity (or the water fluxes from the flow model) and θ the medium's effective porosity. The flow field from the calibrated and validated model is used to calculate CFC concentrations.

The model flow field between the year 2010-10-01 to 2022-10-01 is used. However, the model needs to be extended backwards to allow for modelling in the 1940s when CFCs started to occur in the precipitation and groundwater recharge (Figure 2-2). The complete period of the flow field is recycled to extend the model. The water quality model is set to begin in 1929 with flow from 2010-10-01, even though the CFC emissions begin later. However, starting the model in 1929 results in the flow field for the period of 2010-2022, which is modelled with data from the correct years. Simply, the flow field of 2010-2022 is copied approximately seven times back to 1929.

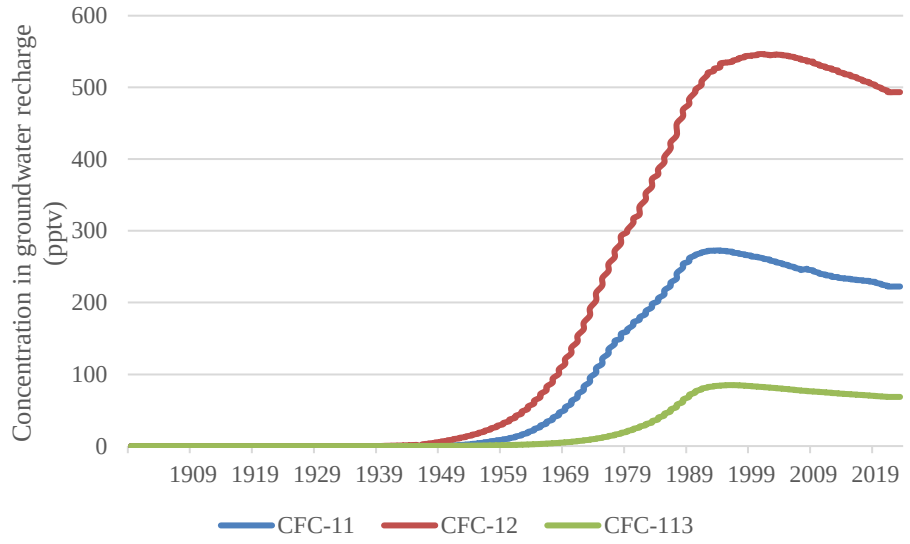

Figure 2-2. *CFC concentrations in groundwater recharge.*

2.3.2 Calibration targets

The final calibrated flow model was used to simulate CFC-12. Since only a few measurements were sampled for each well, the mean error (ME) was evaluated. The calibration goal is to reduce the ME for modelled CFC-12 for each well by re-calibrating the soil properties without impairing the flow calibration results. Wells are placed in the till area, one reaching down into the bedrock. Therefore, the till and bedrock properties are the calibration's focus. To not impair the flow results, the main calibration target is the soil porosity since this parameter does not change the flow results. The horizontal and vertical hydraulic conductivity of the till and bedrock was also evaluated. However, changes to the hydraulic conductivity were only changed on a moderate scale since they can have a major impact on flows and groundwater levels. The calibration mainly focused on improving the CFC results without degrading the flow results since most observations are flow-based (Table 2- 2 and Table 2-3). More specifically, the flow results were to worsen no more than ±5% accumulative error and not exceed a total accumulative error of ±20%. Initial porosity values for the till and bedrock are listed in Table 2-4.

2.4 Groundwater travel time

The methodology to acquire travel times mimics the methodology presented in Jutebring Sterte, et al., 2021. MIKE-SHE particle tracking is used to establish mean groundwater travel times from groundwater recharge to the different wells from which CFC samples have been taken (Table 2-4). Particles are introduced with the groundwater recharge and are, governed by the advection-dispersion equations (Equation 4-6, section 12), transported based on the groundwater flow field. The transportation is based on a pre-calculated transient flow field that can be repeated to extend the time for particle transportation, allowing for long-term transport.

For this investigation, particles were introduced between 2009 to 2022. The model was then run for 1000 years (copying the flow regime of 2009-2022) to capture even very slow-moving groundwater to the different CFC wells. Focusing on the C9 sub-catchments, where the wells are located, approximately 25 particles per 10 mm of recharge were released across the C9-catchment.

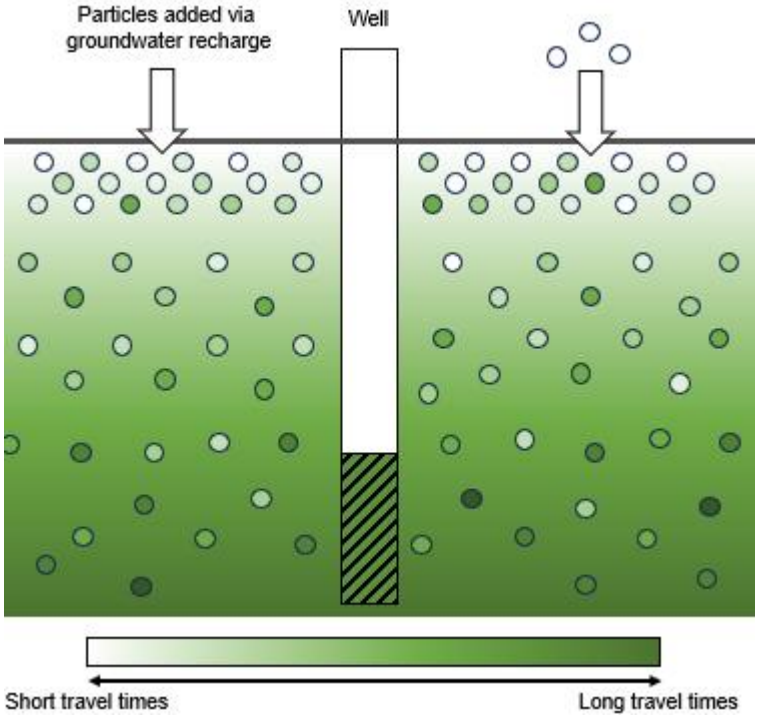

Figure 2-3. *Particles are introduced via the groundwater recharge across the C9-catchent. The travel times for each well are based on the mean travel time it takes for these particles to reach each well filter.*

3 Model calibration results

3.1 Flow and water balance calibration and validation

The model was primarily calibrated towards the flow observations due to the frequency and longevity of flow measurements taken. However, groundwater levels were also considered, with special attention on the SGU wells (101-105) with the most data. The hydraulic conductivity was the focus during the calibration since it has been shown in previous studies to have the greatest impact on the groundwater head and the general water balance. The hydraulic conductivity of the silty sediments was increased from 1×10^{-7} m/s to 5×10^{-7} m/s. The till below 2.5 m was divided into two, with a new deep till at 5 m depth below ground. The new till layer was calibrated to the horizontal hydraulic conductivity of 2×10^{-7} m/s and vertical hydraulic conductivity of 2×10^{-8} m/s (Table 3-3).

After calibration, the general accumulated error was within ±20 %. The correlation coefficient, R, was above 0.8, indicating a strong positive correlation between modelled values and observations. The R^2 coefficient was also high, with values above 0.7 for most sub-stations. No major change in accumulated error or correlation was found during validation, indicating a well-performing model.

Table 3-1 – Table showcasing the statistics for streamflow at each substation before and after calibration (2009-2016) and validation (2009-2022). The table includes the Accumulated error (%) and the correlation coefficients R and R^2 (Equation 1).

	After calibration (2009-2016)			Validation (2009 -2022)		
Flow station	**Acc. error (%)**	**R**	**R^2**	**Acc. error (%)**	**R**	**R^2**
C1	-9.73	0.85	0.68	-10.16	0.87	0.71
C2	12.13	0.88	0.77	8.13	0.88	0.78
C4	-5.97	0.82	0.66	-6.92	0.81	0.64
C5	-0.18	0.85	0.71	-2.30	0.83	0.68
C6	-4.43	0.87	0.74	1.90	0.85	0.70
C7	12.03	0.89	0.79	8.57	0.89	0.79
C9	-5.00	0.92	0.84	-7.73	0.91	0.83
C10	-6.64	0.84	0.70	-12.82	0.79	0.60
C12	4.61	0.91	0.82	-1.48	0.90	0.80
C13	-3.37	0.92	0.83	-4.06	0.91	0.82
C14	13.82	0.87	0.67	12.38	0.87	0.68
C15	-19.22	0.87	0.72	-19.40	0.72	0.48
C16	-10.68	0.89	0.78	-12.26	0.82	0.66
C20	-16.65	0.81	0.50	-16.45	0.80	0.45
Overall abs average	8.89	0.87	0.73	8.90	0.85	0.69

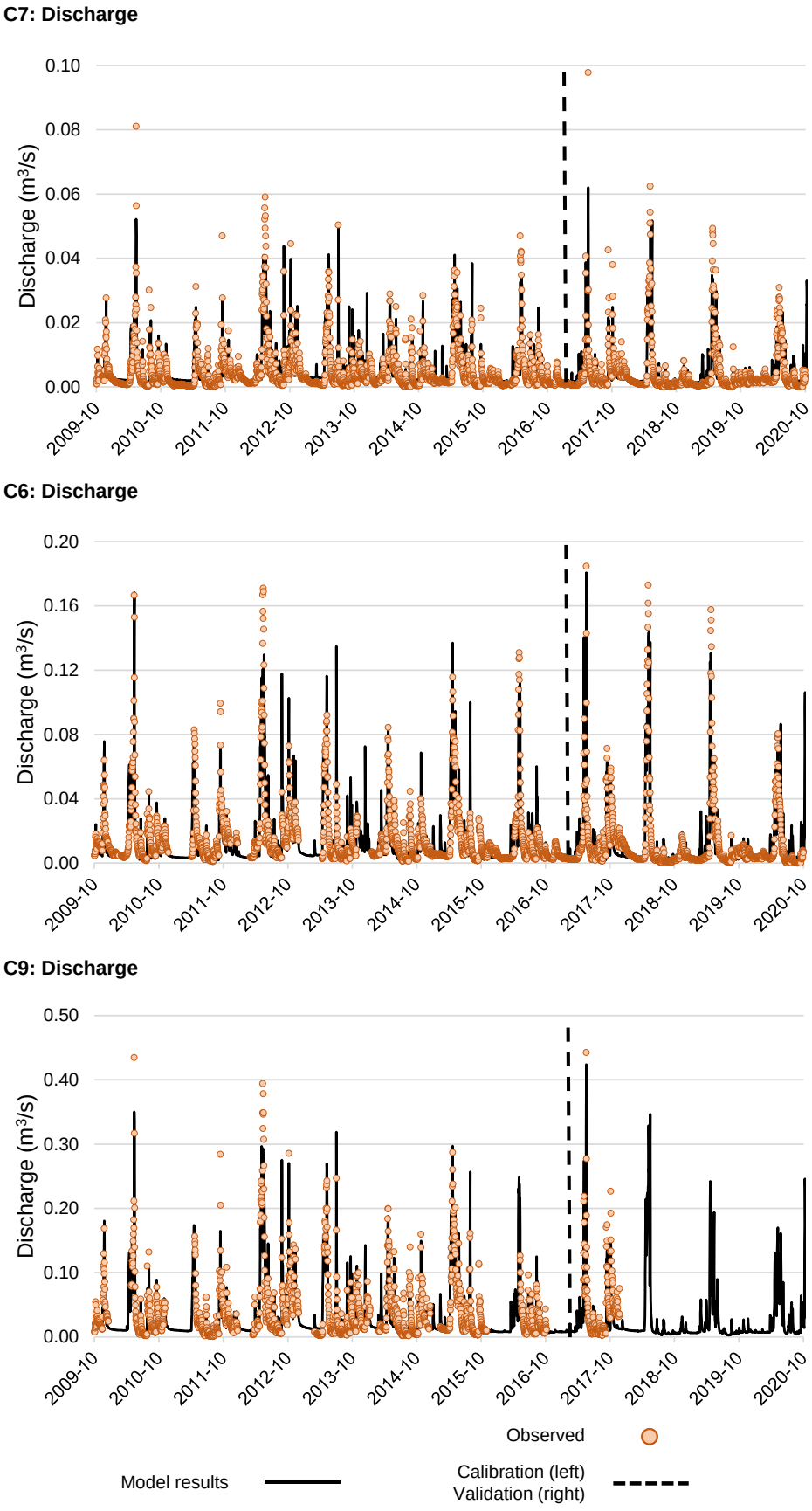

Figure 3-1. *Example of pre and post-calibration flow results for three streams, C7, C6 and C9. Statistics for flow are stated in Table 3-1 for all stream stations. Accumulated flow can be seen for these stations in Figure 3-2.*

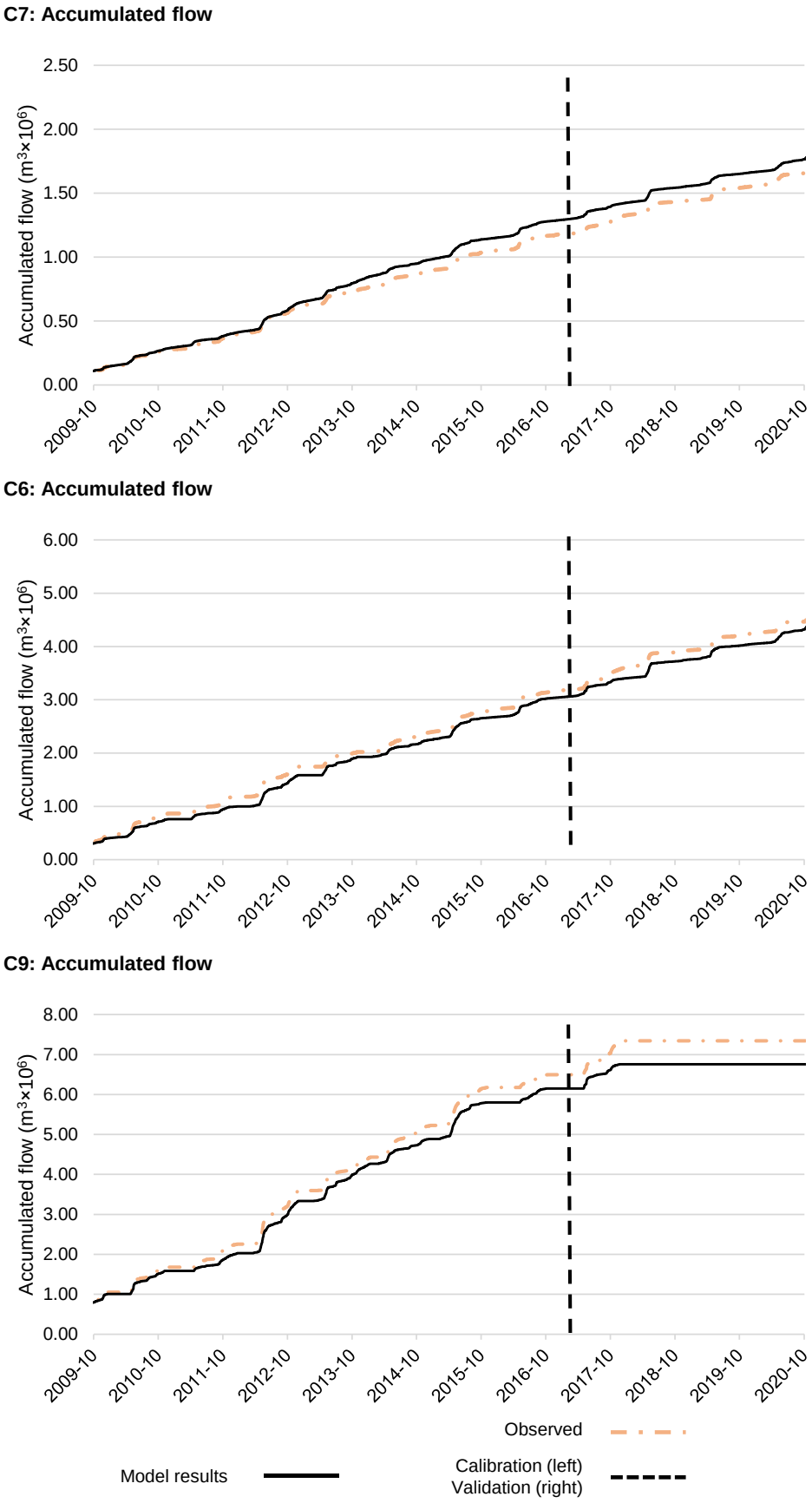

Figure 3-2. *Example of pre and post calibration accumulated flow results for three streams, C7, C6 and C9. Statistics for flow is stated in Table 3-1 for all stream stations.*

The groundwater heads were relatively well represented (Figure 3-3). The best-represented wells are the SGU wells (101-105) with low ME and MAE values (<1) m (Table 3-2). The other wells also had an ME and MAE less than a meter which is deemed acceptable when accounting for the model's horizontal grid size of 50*50 m. For the shallower wells located where the vertical discretization of the model is finer, the error was smaller (less than 1 m for wells 201, 301 and 402). The model resulted in a similarly small ME and MAE for both the validation and calibration period.

Table 3-2 – Table showcasing the statistics for groundwater at each observation well, before and after calibration (2009-2016) and validation (2009-2022). The table includes mean error (ME, Equation 2) and mean absolute error (MAE, Equation 3).

	After calibration (2009 to 2016)		Validation (2009 to 2022)	
Well	**ME (m)**	**MAE (m)**	**ME (m)**	**MAE (m)**
101	0.33	0.37	0.34	0.38
103	-0.95	0.95	-0.98	0.98
104	-0.01	0.16	0.02	0.17
105	0.07	0.23	0.05	0.22
301	0.29	0.29	0.29	0.29
302	0.25	0.25	0.25	0.25
303	0.29	0.29	0.29	0.29
304	0.49	0.49	0.49	0.49
401	0.07	0.26	0.07	0.26
402	0.54	0.54	0.54	0.54
403	0.22	0.29	0.22	0.29
404	0.76	0.76	0.76	0.76
501	0.48	0.48	0.48	0.48
601	0.07	0.09	0.07	0.09
Overall average		0.39		0.39

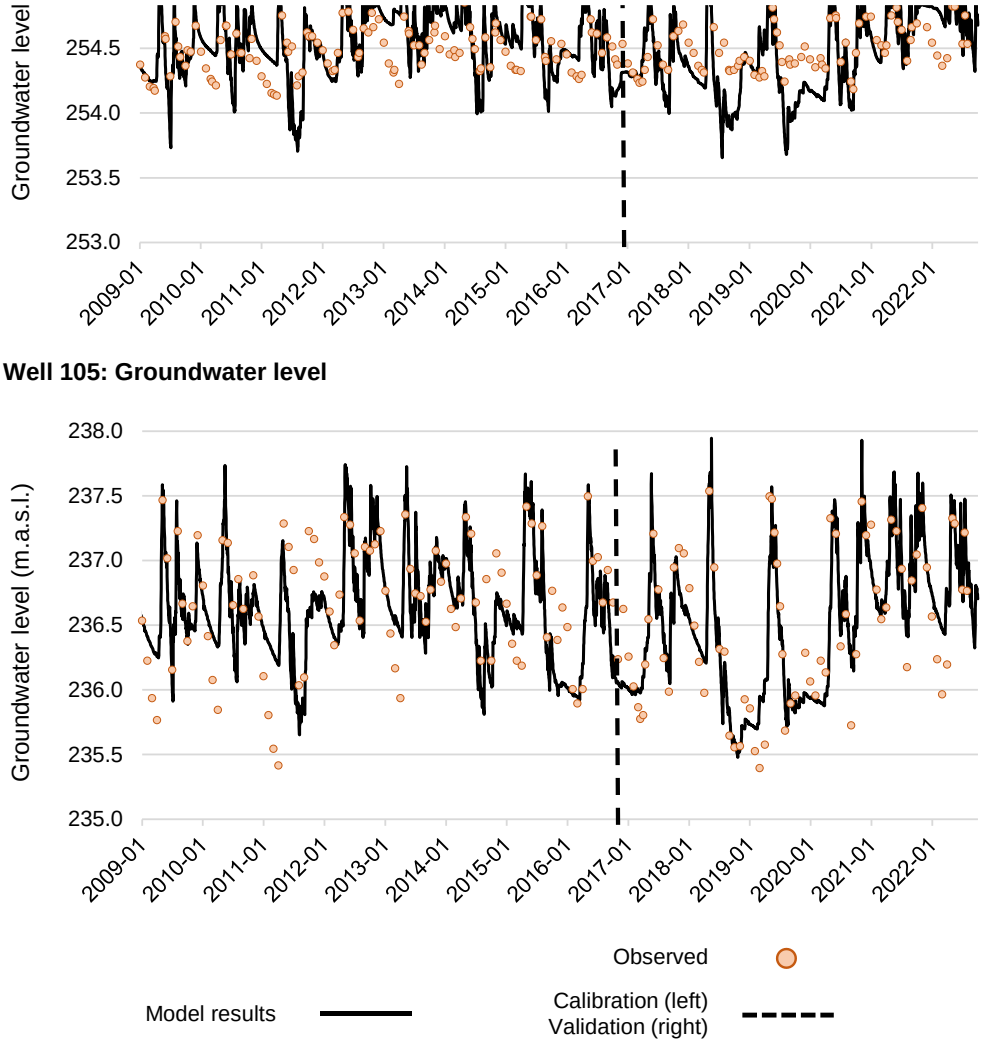

Figure 3-3. *Example of pre and post calibration for groundwater levels for well 104 and 105. Statistics for groundwater level is stated in Table 3-2 and Table 3-1 for all groundwater wells.*

Table 3-3 – Final flow-calibrated parameters for the till and bedrock.

Soil type surface	Depth below ground (m)	Soil type	Horizontal hydraulic conductivity (m/s)	Vertical hydraulic conductivity (m/s)	Porosity
Till	2.5	Till	2×10^{-5}	2×10^{-6}	0.3
	To max soil depth	Mid till	5×10^{-7}	5×10^{-8}	0.3
	Bedrock	Fine till	2×10^{-7}	2×10^{-8}	0.3
	5		1×10^{-9}	1×10^{-9}	0.0001
Peat	7	Peat	1×10^{-5}	5×10^{-5}	0.5
	To max soil depth	Clay	1×10^{-9}	1×10^{-9}	0.55
	Bedrock	Mid till	5×10^{-7}	5×10^{-8}	0.3
	3	Fine till	1×10^{-6}	1×10^{-7}	0.3
	To max soil depth		1×10^{-9}	1×10^{-9}	0.0001
Silty sediments	Bedrock	Silt/clay	5×10^{-7}	5×10^{-7}	0.55
	4	Mid till	5×10^{-7}	5×10^{-8}	0.3
	0.9×max soil depth	Fine till	2×10^{-7}	2×10^{-8}	0.3
	To max soil depth		1×10^{-9}	1×10^{-9}	0.0001
Sandy Sediments	Bedrock	Silt/Sand	2×10^{-5}	2×10^{-5}	0.45
	2.5	Sand	3×10^{-4}	3×10^{-5}	0.35
	To max soil depth	Fine till	2×10^{-7}	2×10^{-8}	0.3
	Bedrock		1×10^{-9}	1×10^{-9}	0.0001

3.2 CFC-12 calibration

The model's calibration using the CFC-12 concentration data followed two steps: calibrating the soil properties without weakening or worsening the model performance and calibrating the soil's porosities. Since all sampled CFC wells were in the till soils or bedrock, the focus was on the till soil properties and the bedrock properties underlying the till soils.

Prior to the recalibration of the model, modelled CFC-12 concentrations were a bit higher than the observed concentrations (ME < 0). In contrast, the modelled concentrations at the deeper wells were a bit low (ME > 0, Figure 3-4). The hydraulic conductivity could be adjusted in the first step to allow for greater solute transport to the deeper wells. However, especially the stream flow rate was found to be quite sensitive to such changes. Therefore, the hydraulic conductivity could only be slightly increased in the deeper part of the till soils and the bedrock without significantly changing the flow calibration (Table 3-4 and Table 3-5).

Porosity is a new parameter added to calculate advective transport on the pre-calculated flow field (Equation 6). When examining the soil porosity, several different porosity combinations could be tested (see Appendix A for some additional calibration examples). In general, the calibration resulted in a mean error of the modelled CFC-12 concentrations at the wells within +/- 100 pptv at almost all well depths (Figure 3-4). The main outlier was the wells at around 15 m depth, where the mean error was greater than 100 pptv.

Although the calibration of the porosities improved the modelled concentrations at these wells, further concentration improvement could not be made without worsening the groundwater level calibration of wells located at other depths. When considering that knowledge regarding the hydraulic properties of the soils at these depths is scarce (few groundwater level measurements, uncertainties in soil depth and bedrock properties, etc.) and considering that there were very few CFC-12 samples in these deeper wells, the CFC calibration did not attempt to better capture CFC-12 concentrations at these depths. However, it may be possible to revisit the CFC calibration and fine-tune the calibration if more data becomes available.

Table 3-4 – Table showcasing the statistics for streamflow at each substation before and after calibration (2009-2016) and validation (2009-2022). The table includes the Accumulated error (%) and the correlation coefficients R and R^2 (Equation 1).

Flow station	Before CFC-12 calibration (2009 to 2022)			After CFC-12 calibration (2009 to 2022)		
	Acc. error (%)	R	R^2	Acc. error (%)	R	R^2
C1	-10.16	0.87	0.71	-12.16	0.87	0.73
C2	8.13	0.88	0.78	0.39	0.88	0.77
C4	-6.92	0.81	0.64	-9.24	0.81	0.64
C5	-2.30	0.83	0.68	-2.09	0.83	0.67
C6	1.90	0.85	0.70	2.11	0.85	0.70
C7	8.57	0.89	0.79	5.51	0.89	0.79
C9	-7.73	0.91	0.83	-8.97	0.92	0.83
C10	-12.82	0.79	0.60	-12.38	0.79	0.60
C12	-1.48	0.90	0.80	-1.78	0.90	0.80
C13	-4.06	0.91	0.82	-4.42	0.91	0.83
C14	12.38	0.87	0.68	12.92	0.87	0.69
C15	-19.40	0.72	0.48	-19.42	0.72	0.47
C16	-12.26	0.82	0.66	-12.43	0.82	0.67
C20	-16.45	0.80	0.45	-16.76	0.80	0.47
Average	8.90	0.85	0.69	8.61	0.85	0.69

Table 3-5 – Final CFC-calibrated parameters for the till and bedrock.

Soil type	Depth below ground (m)	Soil type	Horizontal hydraulic conductivity (m/s)	Vertical hydraulic conductivity (m/s)	Porosity
Till	2.5	Till	2×10^{-5}	2×10^{-6}	0.3
	5	Mid till	5×10^{-7}	5×10^{-8}	0.3
	10	Mid till	5×10^{-7}	5×10^{-8}	0.1
	To bedrock	Fine till	2×10^{-7}	5×10^{-8}	0.05
Bedrock	15	Shallow bedrock	5×10^{-8}	5×10^{-8}	0.01
	50	Mid bedrock	5×10^{-8}	5×10^{-8}	0.001
	100	Deep bedrock	1×10^{-9}	1×10^{-9}	0.0001

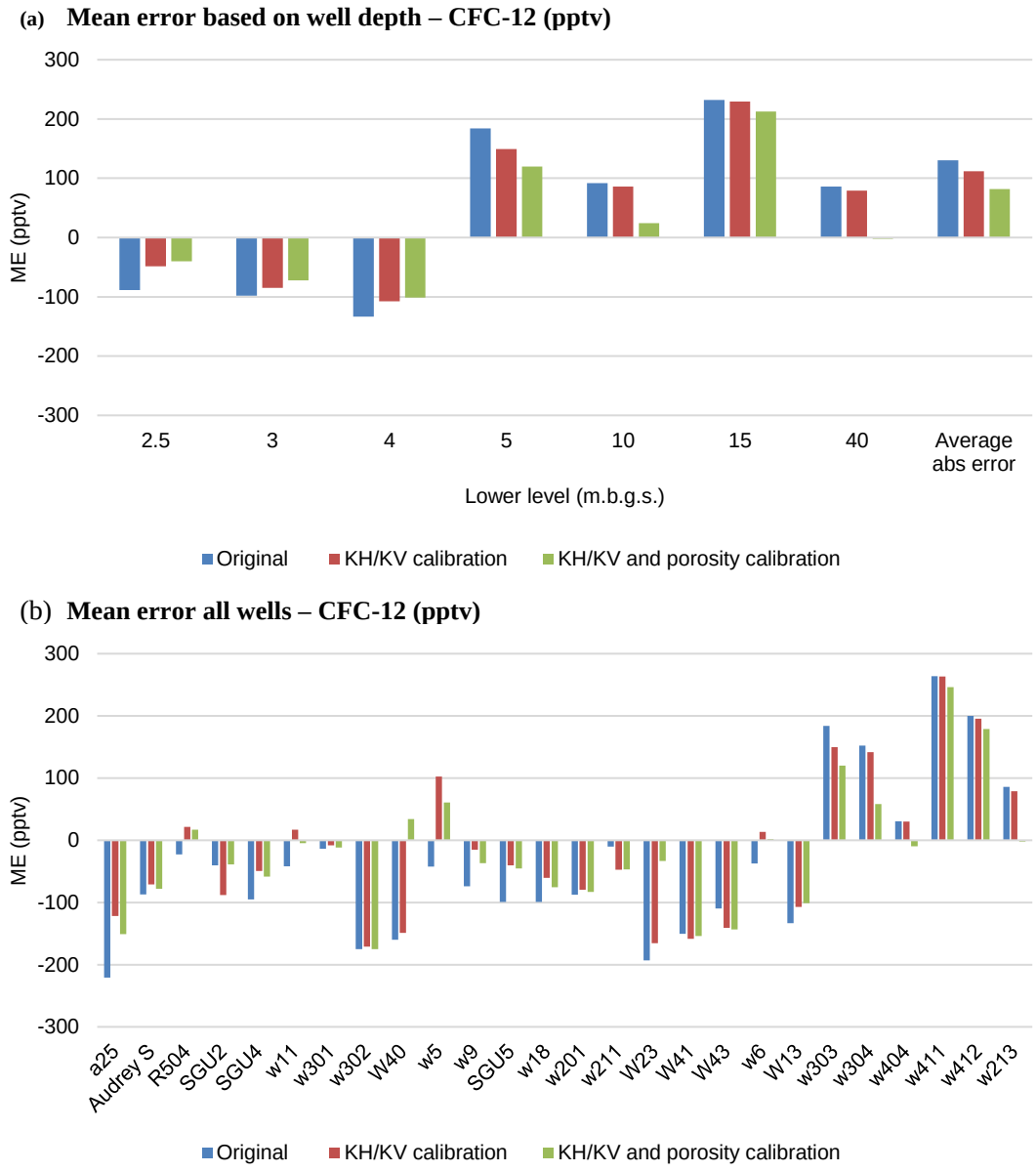

Figure 3-4. *The mean error between sampled and modelled CFC-12 concentration. The figure includes before (original) and after CFC-12 calibration. Here, KH/KV calibration is the first calibration step with changes in hydraulic conductivity, and KH/KV and porosity is the second calibration step, also including changes in porosity (a) The figure shows the general mean error for wells at a certain depth in the model. (b) The figure shows the general mean error for all wells.*

Examples of modelled time-varying concentrations at wells on different depths are showcased in Figure 3-5. The figure showcases the concentration in the groundwater recharge as well as the concentration at the wells over the whole model period. The peak concentration in the groundwater recharge occurs in the late 90s. Shallower wells peak after a couple of years later, depending on the well.

At deeper wells such as w303, w412, and w213, the modelled peak concentration has not yet occurred, and the concentration is still increasing. These wells have a filter depth of about 5, 18 and 48 m, respectively. That they have not yet reached a peak concentration suggests that they are lagging and that it takes longer time for groundwater to reach them compared to shallower wells. After CFC-12 calibration, some of the deeper wells, such as w213 is have come further on its way to peak concentration than before CFC-12 calibration. The results suggest that younger water should most likely reach this well.

However, due to a lack of data at this point in time (one or two observations at each site), it is difficult to determine whether the CFC concentration is increasing naturally or has already reached its maximum concentration and should actually decrease. The current model suggests that the concentration of CFC 12 still increases. Nonetheless, if the concentration actually decreases, the transport times should be much faster.

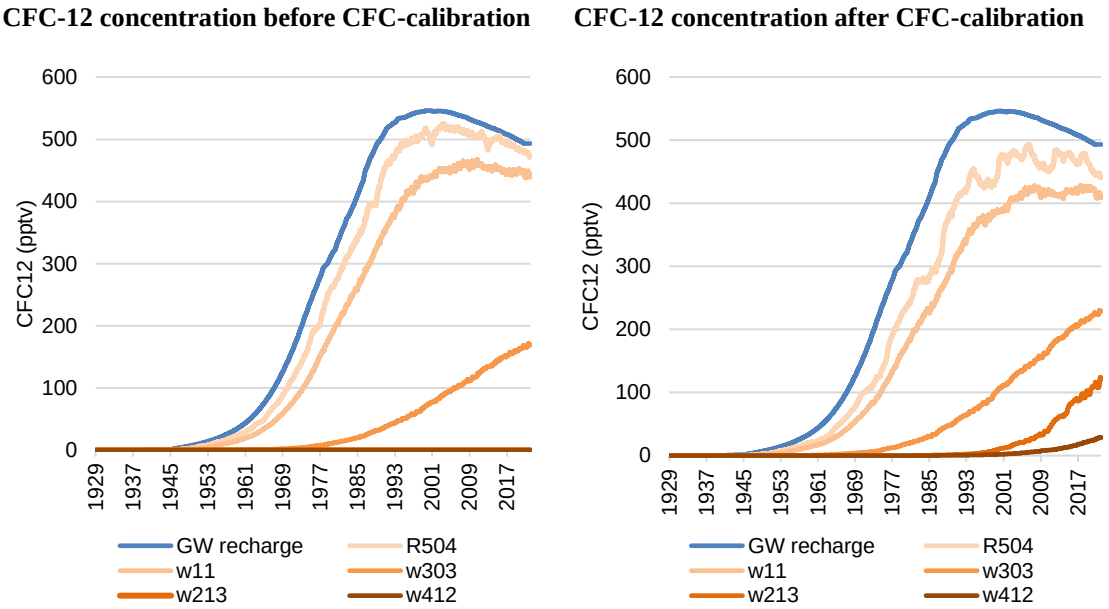

Figure 3-5. *Example of pre and post CFC-12 calibration for some wells. The figure showcases the CFC-12 concentration in the groundwater at the wells and the concentration in the groundwater recharge.*

4 Groundwater travel time

Particle tracking was applied to establish travel times to each well before and after model calibration using CFC-12 (further described in section 2.4). Mean travel times (MTT), geometric mean and median travel times are displayed in Table 4-1, section 4.1. Histograms showing the number of particles as well as their general travel time distribution examples are shown in Figure 4-4, section 4.1. Result figures for the other wells can be found in Appendix B. A comparison between travel time results and sampling location are shown in the section 4.2.

4.1 Travel time results and distribution

In till soils, the main water transportation occurs in the shallow part of the soil. Shallower wells therefore, received more particles than deeper wells since the particle release was recharge-weighted (more particles equal to greater flow rotation, section 2.4). Wells receiving water mainly from shallow soils also receive more particles. These particles tend to have shorter travel times, while in general, deeper wells receive fewer particles with longer travel times (Figure 4-4). Since the deeper wells receive fewer particles, the summary statistics calculated at these wells are much more sensitive to the travel times of the few particles that reach them.

The MTT calculated using the arithmetic mean of the travel times of all particles reaching a specific well is very sensitive to the tail of the travel time distribution. One single particle with a travel time much greater than the rest of the distribution can skew the travel time to much greater MTTs than the bulk of particles suggests (Jutebring Sterte, et al., 2021a). The median and the geometric mean tend to give a better representation of the travel times of the bulk of particles and are less impacted by a few particles with long travel times. Considering this, finding a more significant change in MTTs than in the median and geometric mean before and after CFC-12 calibration is unsurprising.

The main changes of the model pre-post-calibration were an increase in the vertical hydraulic conductivity of the deeper till soils and bedrock and a change in the porosity. These changes did not significantly impact the flow model results but impacted the timing and concentration of the CFC-12 at the wells. The changes also impacted the travel times to the wells.

The shallower wells generally received a couple of years shorter MTTs, while the median stayed the same or similar. In general, the shallow wells received a comparable proportion of particles with short and long travel times but fewer particles with very long travel times, which affects the MTT more than the median (Figure 4-4, Figure 4-2, Table 4-1).

Table 4-1 – Modelled travel time results. The table includes the mean, geometric mean (geo-mean), and median travel times of particles to each well before and after CFC calibration, as well as the sampled CFC-12 concentration. Note that the data presented in the "Before CFC-12 calibration" and the "After CFC-12 calibration" columns of the table are outputs from MIKE SHE and the decimal precision of this data is not necessarily relevant given the precision of the infiltrating CFC-12 concentrations used in the modelling.

				Before CFC-12 calibration			After CFC-12 calibration		
	Depth of calc.-layer	No of samples	Average CFC-12 (pptv)	MTT (years)	Median (years)	Geo-mean (years)	MTT (years)	Median (years)	Geo-mean (years)
a25	2.5	1	269.3	0.19	0.00	0.01	0.19	0.00	0.00
Audrey S	2.5	1	378.4	2.55	0.00	0.02	1.24	0.00	0.01
R504	2.5	1	464.1	1.81	0.00	0.04	1.33	0.00	0.02
SGU2	2.5	2	413.0	0.45	0.06	0.04	0.40	0.00	0.02
SGU4	2.5	2	358.3	16.50	0.09	0.07	10.16	0.14	0.06
w11	2.5	1	413.8	15.09	0.00	0.04	2.74	0.00	0.02
w301	2.5	1	445.4	2.55	0.00	0.02	1.24	0.00	0.01
w302	2.5	2	284.0	2.55	0.00	0.02	1.24	0.00	0.01
w40	2.5	1	324.5	0.42	0.00	0.03	0.82	0.00	0.02
w5	2.5	1	397.6	35.18	0.03	0.11	4.95	0.00	0.03
w9	2.5	1	375.5	15.09	0.00	0.04	2.74	0.00	0.02
SGU5	3.0	1	455.3	0.44	0.00	0.04	0.41	0.00	0.02
w18	3.0	1	356.1	21.21	0.12	0.07	2.63	0.11	0.04
w201	3.0	2	405.5	0.28	0.00	0.02	0.27	0.00	0.01
w211	3.0	1	462.6	3.19	0.97	0.89	1.82	0.87	0.71
w23	3.0	1	286.4	0.30	0.00	0.03	0.59	0.00	0.02
w41	3.0	2	372.0	0.28	0.00	0.02	0.27	0.00	0.01
w43	3.0	1	385.7	5.97	0.74	0.85	3.27	0.68	0.65
w6	3.0	1	418.4	192.98	73.86	54.77	38.13	26.24	19.99
w13	4.0	1	362.0	0.00	0.00	0.00	0.01	0.00	0.00
w303	5.0	2	336.2	155.82	82.60	86.63	56.17	39.88	41.71
w304	10	2	155.3	325.01	267.10	269.91	78.79	73.54	69.60
w404	10	2	31.1	574.25	541.39	533.07	127.91	131.01	124.84
w411	15	1	263.8	1278.61	1250.50	1260.60	101.28	97.20	98.69
w412	15	2	200.0	1278.61	1250.50	1260.60	101.28	97.20	98.69
w213	40	1	85.9	695.50	623.78	675.96	57.87	56.12	57.63

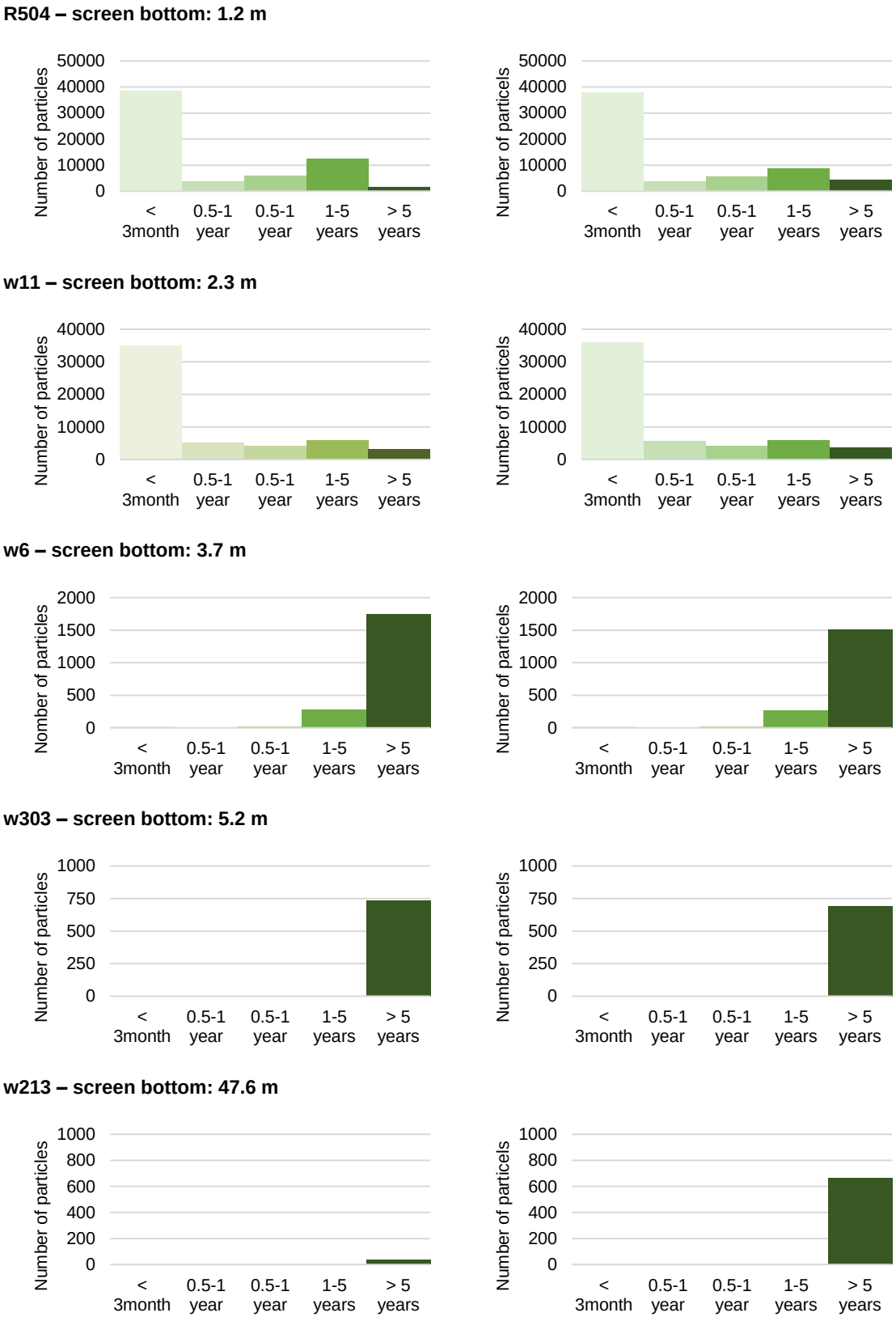

Figure 4-1. *Example of pre- and post-distribution of travel times for some example wells at different depths, beginning with shallower wells. Pre-calibration results to the left and post calibration to the right. R504 and w11 are examples of shallower wells at 2-3 m depth, with corresponding shorter travel times. In comparison, w303 and w213 are deeper located wells at 5 and 40 m.b.g., respectively, with longer travel times.*

4.2 Travel times and CFC sampling

After CFC-12 calibration, a stronger connection between travel times and CFC-12 samples can be seen for both mean, median and geometric mean travel times (Figure 4-1). R^2 values increase from about 0.38 (indicating a weak correlation) to about 0.60 (indicating a moderate correlation) after CFC-12 calibration. The travel times decrease with CFC-12 concentration, indicating a greater dilution of CFC-12 at larger depths.

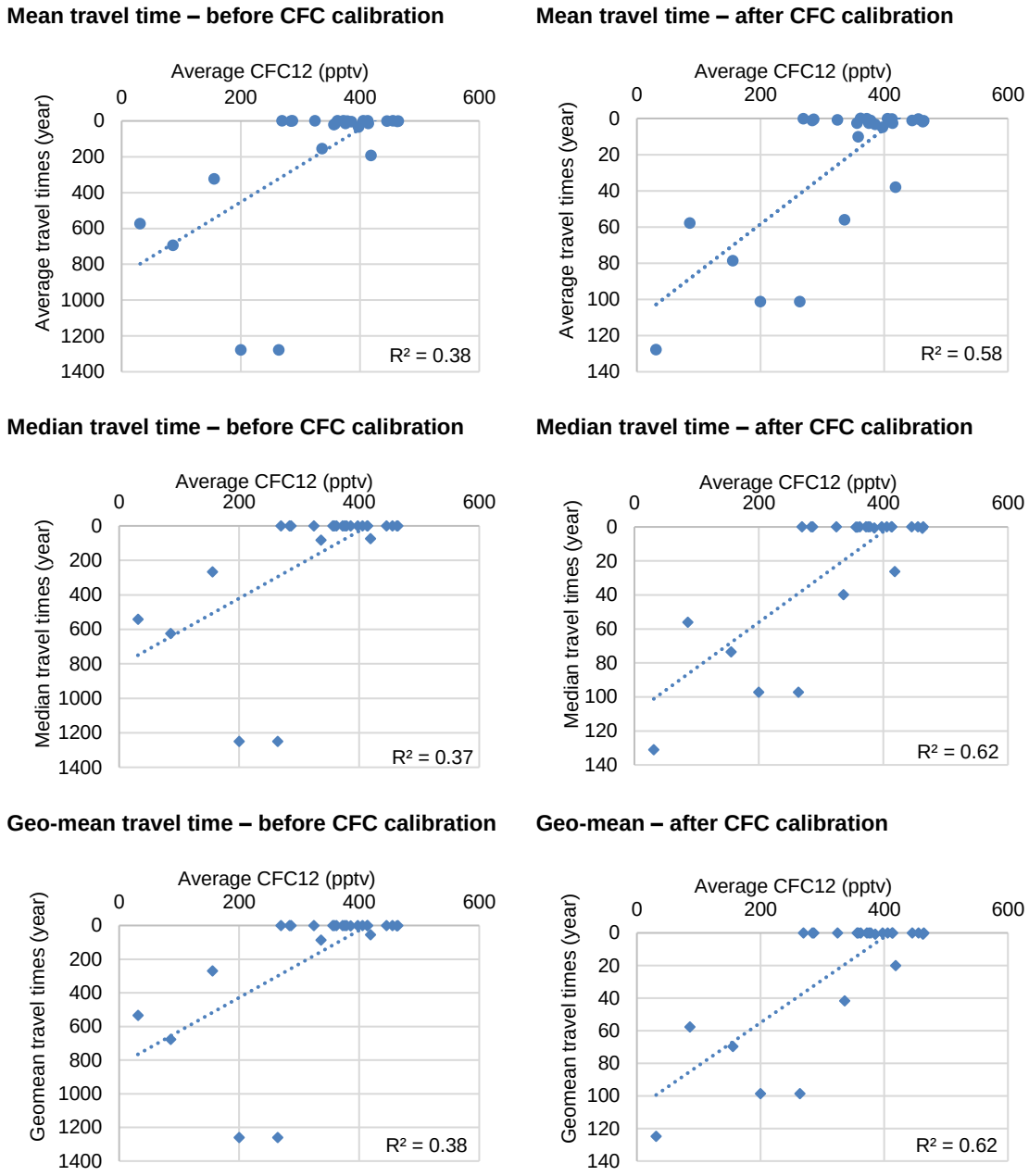

Figure 4-2. *Mean, median and geometric mean of particle travel times in years (x-axis) and average CFC-12 concentration in pptv (x-axis) for each well. The figure showcases before (left) and after (right) CFC-12 calibration.*

It can also be discussed what to compare the MIKE SHE particle travel times with. In MIKE SHE, particle tracing is only allowed in the saturated zone. Although the results may not fully describe occasions of intermixing of water stored in the unsaturated zone or overland water, the modelled travel times seems to well describe the baseflow part of groundwater. Such occasions of intermixing are more likely to occur at shallow-located wells or streams during snowmelt or intense rain situations. Thereby, it's likely a better connection between MIKE SHE particle tracking results and water quality samples occurring during dry or winter seasons, at least for shallow wells and streamflow, when groundwater recharge rates are generally rather low.

The CFC-12 samples taken so far have been taken during the spring, summer, and autumn seasons. Two trials were conducted to test the theory that particle tracking results are better connected to dry or winter seasons. One where all samples during the spring snowmelt and shortly after a rain event were removed for the shallow wells (well less than 3m deep, first row Figure 4-3) and one where the shallow wells were removed completely (second row Figure 4-3).

In the first row, the correlation increased both before (0.38 to 0.46) and after CFC-12 calibration (0.62 to 0.77). However, when only looking at the deeper wells (second row), there is no correlation before the CFC-12 calibration, while after the calibration, the R^2 correlation is moderate (0.46). The calibration results show a possible connection between CFC-12 and MIKE SHE particle travel times, which is more robust when looking at dry or winter seasons. Future investigations with winter samples would be of interest in the future at least if groundwater travel times of the saturated zone should be used.

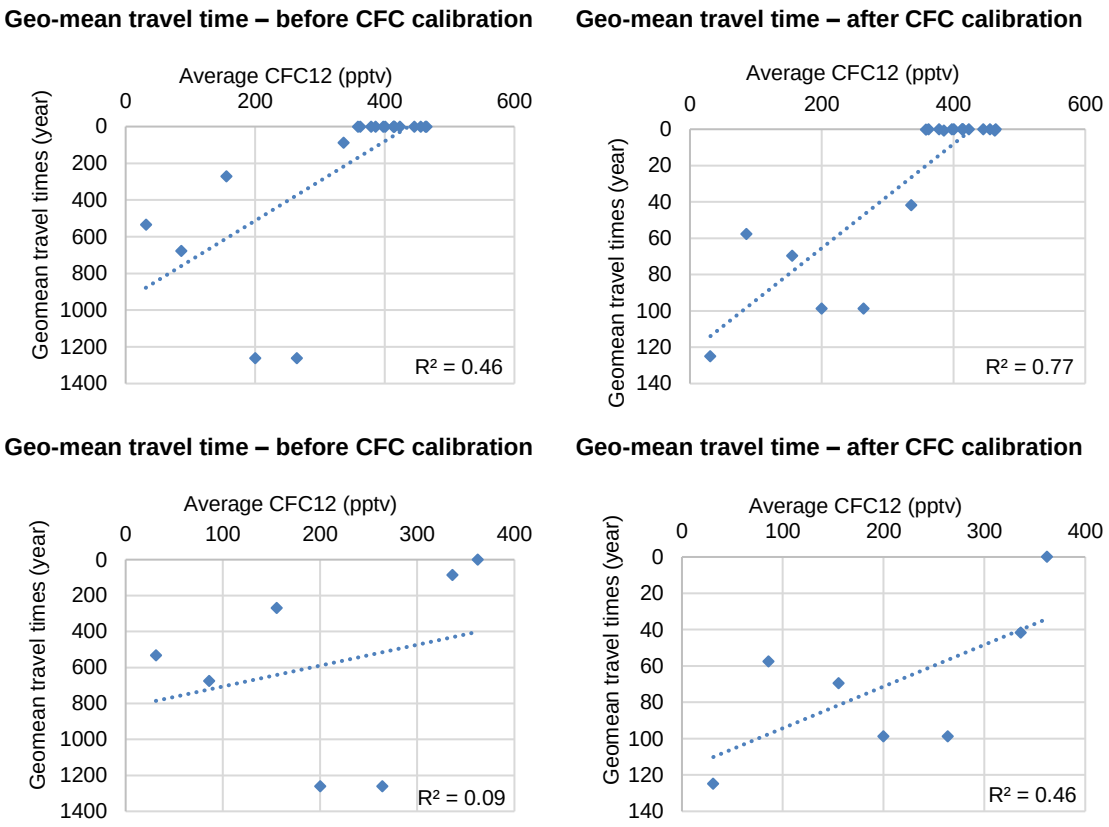

Figure 4-3. *Mean, the median and geometric mean of particle travel times in years (x-axis) and average CFC-12 concentration in pptv (x-axis) for each well. The figure showcases before (left) and after (right) CFC-12 calibration.*

5 Discussion

Flow models often uses streamflow and groundwater heads to calibrate soil properties. These are useful calibration tools that often gives a good representation of hydraulic conductivities across a catchment. However, when hydrological models are used to assess travel times and solute transport, the porosity of the soils must be accounted for. Such data can be very sparse and often a standard value is used. One approach to assessing the transport-related parameters of a hydrological model is to use a tracer solute. An ideal solute for tracing purposes is non-reactive with the surrounding environment and exhibits detectable natural amplitude changes over time. Isotopes, such as oxygen-18 is a common tool. However, due to amplitude dampening affects, it may not be tracible after about 5 years (Kirchner, 2016). In this pilot study, CFC-12 was tested as a tracer solute, which potentially have a traceability of about 30-50 years. Results show that calibrating the MIKE SHE models porosities against CFC-12 increases the connection between MTT and CFC-12 concentration (Figure 10-1, section 4.2). This highlights the potential to use CFCs to calibrate the models' porosities. However, there are uncertainties to consider with the current model set up as well as the CFC 12 sampling.

Currently, it isn't easy to evaluate both the model and the samples themselves on just one or two samples per well, creating both spatial and temporal uncertainties. For example, with only a few measurements, it's difficult to assess if a measurement point is an outlier or if it is characteristic of CFC concentrations at that depth. It is also difficult to interpret whether the CFC-12 concentration increases or decreases over time. Lack of data at different depths and for different soils may also result in difficulties to assess the model outputs with regards to soil layering and spatial variations. For now, most samples have been taken in till soils at shallow depths, resulting in that other parts of the catchment with other soil properties cannot be evaluated at this point in time. All these temporal and spatial uncertainties, can have a profound impact on the curve-fitting calibration processes, resulting in very different results in groundwater travel times, especially at larger depths where concentrations might be lagging relative the shallow wells and may not have reached the CFC-peak concentration (Figure 3-5, section 3.2). At this point, it is not possible to validate the model for another period, so modelled CFC-12 predictions are uncertain. Therefore, the current CFC-12 calibration should be evaluated under caution and not presumed to be more accurate than before the CFC calibration it at its current stage. However, with more samples, the model calibration could be made more accurately, and then the travel time evaluation could be re-made.

The current grid size of 50×50m might not be enough to capture the CFC-12 variation in the groundwater across the catchment. Groundwater samples are point samples that can be very sensitive to the specific location they have been sampled and may not be representative of the general properties of the catchment. Since the CFC-12 concentration is applied in the groundwater recharge, it's crucial that the first calculation layer is deep enough to include the top of the phreatic surface, i.e. the groundwater table, to get correct concentration calculations in MIKE SHE. A smaller grid size could allow for the implementation of a shallower first calculation layer which could better account for areas with relatively high groundwater tables, e.g. the riparian zone along the streams. Since the till has such a great exponential decrease in hydraulic conductivity, especially at shallower depth, the current grid discretization might not be fine enough to capture variations in CFC concentrations that can be seen between 0.5-2m depth. A smaller grid size and more samples would allow for better-modelled CFC representation. A smaller grid size would require a smaller local model domain, but the larger Krycklan model could still be used to provide boundary conditions for a nested, local model.

There are also uncertainties regarding soil depth and deep soil properties. Another way to examine the model's ability to represent CFC concentrations is to instead calibrate the model against measured CFC concentrations in the stream. The stream concentration represents a sum of the upstream properties and can provide a better understanding of the overall functioning of the catchment and give a better overview of the general soil properties. Having observations from outlets of several catchments with different sizes and characteristics might be beneficial, especially on larger model scales. Groundwater samples can then provide additional information, validation points, or a soil depth perspective. However, in both cases, times series with at least monthly or by-weekly samples would be necessary to better understand the CFCs within a catchment.

6 Conclusions

This study examined the added value of CFC concentration data when calibrating a MIKE SHE hydrological model. Conclusive results regarding the added value of the CFC data during the calibration process were difficult to evaluate due to the temporally and spatially sparse CFC data available. However, results from this study indicate that CFCs could be a useful tool for calibrating model porosities thus providing greater confidence in modelling results when the hydrological model is used to examine pollutant transport assuming the spatial and temporal resolution of the CFC data was sufficient. However, due to the lack of CFC observations in deeper soils (> 2m deep) and the limited temporal resolution of the samples in this study, it was not possible to discern whether the hydrological model was able to adequately represent solute travel times as it could not be determined if the peak CFC concentration at the sampling locations had occurred yet. In order to fully utilize CFC data in model calibration in the instance of this study, longer CFC concentration time-series are needed with an increased regularity.

7 Acknowledgement

This report has been made possible by the Swedish Infrastructure for Ecosystem Science (SITES), in this case at the Krycklan Catchment. SITES receives funding through the Swedish Research Council under grant no 2017-00635.

8 References

SKB's (Svensk Kärnbränslehantering AB) publications can be found at www.skb.com/publications.

Bishop K, Seibert J, Nyberg L, Rodhe A, 2011. Water storage in a till catchment. II: Implications of transmissivity feedback for flow paths and turnover times. Hydrol. Process., Volume 25, p. 3950–3959.

Bosson E, Sassner M, Sabel U, Gustafsson L-G, 2010. Modelling of Present and Future Hydrology and Solute Transport at Forsmark. SKB R-10-02. Svensk Kärnbränslehantering AB.

Bosson E, Gustafsson L-G, Sassner M, 2008. Numerical Modelling of Surface Hydrology and Near-Surface Hydrogeology at Forsmark. SKB R-08-09. Svensk Kärnbränslehantering AB.

Burns D A, Plummer L N, McDonnell J J, Busenberg E, Casile G C, Kendall C, Hooper R P, Freer J E, Peters N E, Beven K, Schlosser P, 2003. The Geochemical Evolution of Riparian Ground Water in a Forested Piedmont Catchment. Groundwater, Volume 41, p. 913–925.

Cardenas M B, 2007. Potential contribution of topography-driven regional groundwater flow to fractal stream chemistry: Residence time distribution analysis of Tóth flow. Geophysical Research Letters, 35(5), p. L05403.

Chambers L A, Gooddy D C, Binley A M, 2019. Use and application of CFC-11, CFC-12, CFC-113 and SF6 as environmental tracers of groundwater residence time: A review. Geoscience Frontiers, 10(5), pp. 1643-1652.

Cook P, Solomon D, 1997. Recent advances in dating young groundwater: chlorofluorocarbons, 3H3He and 85Kr. Journal of Hydrology, Volume 191, pp. 245-265.

Darling W G, Gooddy D C, MacDonald A M, Morris B L, 2012. The practicalities of using CFCs and SF6 for groundwater dating and tracing. Applied Geochemistry, 27(9), pp. 1688-1697.

DHI, 2023. MIKE SHE User Guide and Reference Manual. [Online] Available at: https://manuals.mikepoweredbydhi.help/2023/MIKE_SHE.htm#More_Information [Accessed 14 04 2023].

DHI, 2024. Integrated catchment hydrological modelling MIKE SHE. [Online] Available at: https://www.dhigroup.com/technologies/mikepoweredbydhi/mike-she [Accessed 11 08 2024].

Goller R, Wilcke W, Leng M J, Tobschall H J, Wagner K, Valarezo C, Zech W, 2005. Tracing water paths through small catchments under a tropical montane rain forest in south Ecuador by an oxygen isotope approach. Journal of Hydrology, 308(1-4), pp. 67-80.

Graham D N, Butts M B, 2005. Flexible, integrated watershed modelling with MIKE SHE. Watershed models, pp. 245-272, CRC Press.

Jasechko S, Perrone D, Befus K M, Bayani Cardenas M, Ferguson G, Gleeson T, Luijendijk E, McDonnell J J, Taylor R G, Wada Y, Kirchner J W, 2017. Global aquifers dominated by fossil groundwaters but wells vulnerable to modern contamination. Nature Geoscience, 10(6), p. 425–429.

Jutebring Sterte E, Johansson E, Sjöberg Y, Karlsen R H, Laudon H, 2018. Groundwater-surface water interactions across scales in a boreal landscape investigated using a numerical modelling approach. Journal of Hydrology, Volume 560, pp. 184-201.

Jutebring Sterte E, Lidman F, Lindborg E, Sjöberg Y, Laudon H, 2021a. How catchment characteristics influence hydrological pathways and travel times in a boreal landscape. Hydrol. Earth Syst. Sci., Volume 25, p. 2133–2158.

Jutebring Sterte E, Lidman F, Balbarini N, Lindborg E, Sjöberg Y, Selroos J O, Laudon H, 2021b. Hydrological control of water quality–Modelling base cation weathering and dynamics across heterogeneous boreal catchments. Science of the Total Environment, Volume 799, p. 149101.

Karlsen R H, 2016. Spatiotemporal streamflow variability in a boreal landscape, Uppsala: Diss. Acta Universitatis Upsaliensis.

Karlsen R H, Grabs T, Bishop K, Buffam I, Laudon H, Seibert J, 2016. Landscape controls on spatiotemporal discharge variability in a boreal catchment. Water Resources Research, 52(8), p. 6541–6556.

Kazemi G A, Lehr J H, Perrochet P, 2006. Groundwater age. s.l.:John Wiley & Sons.

Kim K, Shon Z, Nguyen H, Jeon E, 2011. A review of major chlorofluorocarbons and their halocarbon alternatives in the air. Atmospheric environment, Volume 45, pp. 1369-1382.

Kirchner J W, 2016. Aggregation in environmental systems – Part 1: Seasonal tracer cycles quantify young water fractions, but not mean transit times, in spatially heterogeneous catchments. Hydrol. Earth Syst. Sci., Volume 20, p. 279–297.

Kolbe T, Bishop K, 2024. Estimating groundwater and stream water ages with chlorofluorocarbons. SKB P-24-07 Svensk Kärnbränslehantering.

Kolbe T, Marçais J, de Dreuzy J R, Labasque T, Bishop K, 2020. Lagged rejuvenation of groundwater indicates internal flow structures and hydrological connectivity. Hydrological Processes, Volume 34, p. 2176–2189.

Kralik M, 2015. How to Estimate Mean Residence Times of Groundwater. Proced. Earth Plan. Sc., Volume 13, p. 301–306.

Laudon H, 2020. Snowcat groundwater monitoring. [Online] Available at: https://www.safedeposit.se/projects/235 [Accessed 04 12 2023].

Laudon H, Taberman I, Ågren A, Futter M, Ottosson-Löfvenius M, Bishop K, 2013. The Krycklan Catchment Study – a flagship infrastructure for hydrology, biogeochemistry, and climate research in the boreal landscape. Water Resour. Res., Volume 49, p. 7154–7158.

Laudon, H, Hasselquist E M, Peichl M, Lindgren K, Sponseller R, Lidman F, Kuglerová L, Hasselquist N J, Bishop K, Nilsson M B, Ågren A M, 2021. Northern landscapes in transition: evidence, approach and ways forward using the Krycklan Catchment Study. Hydrol. Process., 35(4), p. e14170.

McDonnell J J, McGuire K, Aggarwal P, Beven K, Biondi D, Destouni G, Dunn S, James A, Kirchner J, Kraft P J H P, Lyon S, 2010. How old is streamwater? Open questions in catchment travel time conceptualization, modelling and analysis. Hydrol. Process., Volume 24, p. 1745–1754.

Neupane A, Raj N, Deo R, Ali M, 2021. Development of data-driven models for wind speed forecasting in Australia. In: Predictive modelling for energy management and power systems engineering. s.l.:Elsevier, pp. 143-190.

Nyberg L, 1995. Water flow path interactions with soil hydraulic properties in till soil at Gårdsjön, Sweden. J. Hydrol., Volume 170, p. 255–275.

Peralta-Tapia A, Sponseller R A, Ågren A, Tetzlaff D, Soulsby C, Laudon H, 2015. Scale-dependent groundwater contributions influence patterns of winter baseflow stream chemistry in boreal catchments. Journal of Geophysical Research: Biogeosciences, 120(5), pp. 2169-8953.

Plummer L N, Bussenberg E, 2000. CHLOROFLUOROCARBONS. In Peter G. Cook, Andrew L. Herczeg (Eds.): Environmental Tracers in Subsurface Hydrology. Bosont, MA, s.l.: Springer US, pp. 441-478.

Sprenger M, Tetzlaff D, Buttle J, Laudon H, Soulsby C, 2018. Water ages in the critical zone of long-term experimental sites in northern latitudes. Hydrol. Earth Syst. Sci, Volume 22, p. 3965–398.

Stockinger M P, Bogena H R, Lücke A, Stumpp C, Vereecken H, 2019. Time variability and uncertainty in the fraction of young water in a small headwater catchment. Hydrol. Earth Syst. Sci., Volume 23, p. 4333–4347.

Svartberget Field Research Station, 2023. Water balance - stream water level [Data set]. [Online] Available at: https://data.fieldsites.se/

Sveriges geologiska undersökning (SGU), 2022. Kartvisare och diagram för mätstationer. [Online] Available at: https://www.sgu.se/grundvatten/grundvattennivaer/matstationer/ [Accessed 23 11 2022]. (In Swedish)

Swedish Geological Survey (SGU), 2016. Soil depth to bedrock map. [Online] Available at: https://www.sgu.se/en/products/maps [Accessed April 18 2016].

Tejshree T, 2023. Krycklan Data Services. [Online] Available at: https://www.slu.se/en/departments/forest-ecology-management/environment/krycklan/data/ [Accessed 26 01 2023].

Tetzlaff D, Soulsby C, 2008. Sources of baseflow in larger catchments – Using tracers to develop a holistic understanding of runoff generation. J. Hydrol. Volume 359, p. 287–302.

von Freyberg J, Allen S T, Seeger S, Weiler M, Kirchner J Wa, 2018. Sensitivity of young water fractions to hydro-climatic forcing and landscape properties across 22 Swiss catchments. Hydrol. Earth Syst. Sci, Volume 22, p. 3841–3861.

Werner K, Sassner M, Johansson E, 2013. Hydrology and Near-Surface Hydrogeology at Forsmark – Synthesis for the SR-PSU Project. R-13-19. Svensk Kärnbränslehantering AB.

9 Appendix A

CFC-12 calibration additional results

Additional CFC-12 calibration results. This section showcases some CFC-12 calibration results depending on porosity at different soil depths. The calibration examples are shown in Table 9-1and the resulting men error at different soil depths are shown in Figure 9-1.

Table 9-1 – CFC-12 calibration examples. Calibration examples of porosity impact at a certain depth. The resulting mean error for each example is shown in Figure 9-1. KH/KV and porosity calibration is the final calibration on which later groundwater travel times were evaluated.

				Example					
		Original	KH/KV and porosity calibration	1	2	3	4	5	6
Till	2.5	0.3	0.3	0.4	0.1	0.3	0.3	0.3	0.3
	5	0.3	0.3	0.4	0.1	0.1	0.3	0.3	0.3
	10	0.3	0.1	0.05	0.05	0.05	0.1	0.1	0.1
	To bedrock	0.3	0.05	0.05	0.05	0.05	0.05	0.05	0.3
Bedrock	5	0.01	0.1	0.1	0.1	0.1	0.01	0.1	0.1
	15	0.01	0.01	0.01	0.01	0.01	0.01	0.1	0.01
	50	0.0001	0.001	0.001	0.001	0.001	0.001	0.01	0.001
	100	0.0001	0.0001	0.0001	0.0001	0.0001	0.0001	0.001	0.0001

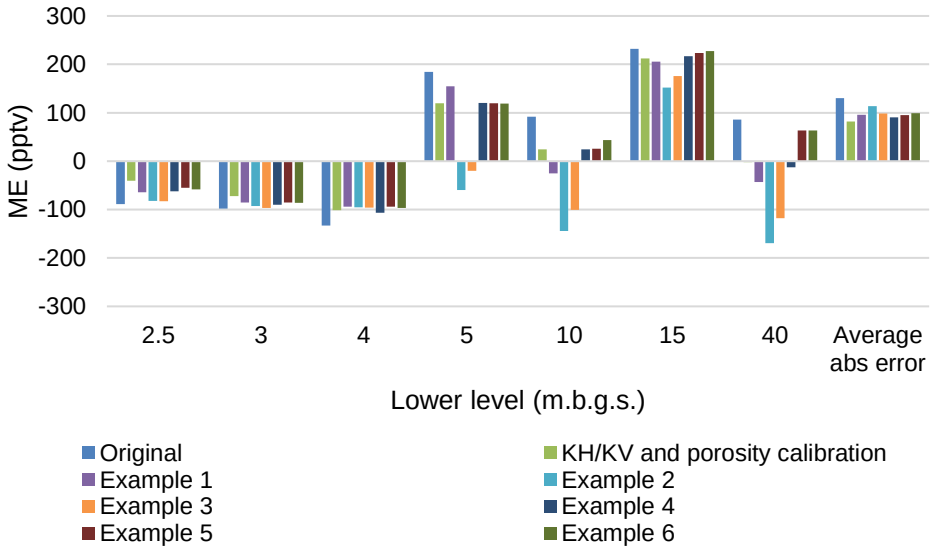

Figure 9-1. *The mean error between sampled and modelled CFC-12 – concentration. The figure includes before (original) and after CFC-12 calibration. The examples are described in Table 9-1 and mainly showcases the impact of porosity changes.*

10 Appendix B

Travel times - all wells.

Groundwater travel time results for all wells (Table 2-4). This section showcases the travel time distribution of the particle tracking results, pre and post-CFC12-calibration Figure 10-1.

Travel time distribution of particles

Before CFC-12 calibration

a25 – MTT: 0.19 y. Median: 0.00 y

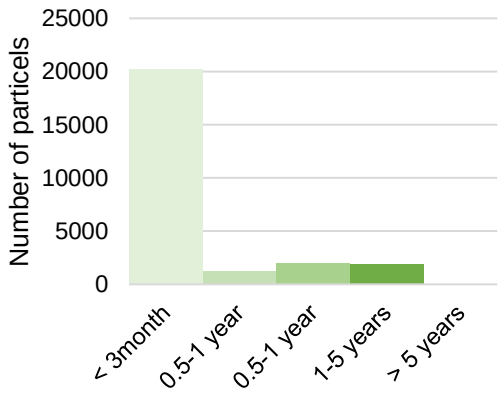

Audrey S –: 2.55 y. Median: 0.00 y

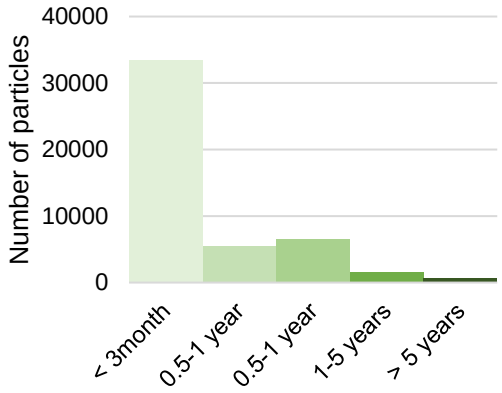

R504 – MTT: 1.81 y. Median: 0.00 y

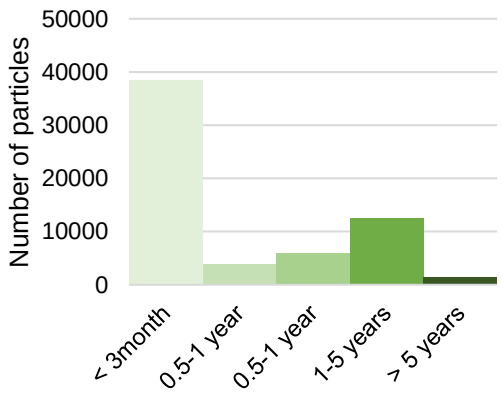

Travel time distribution of particles

After CFC-12 calibration

a25 – MTT: 0.19 y. Median: 0.00 y

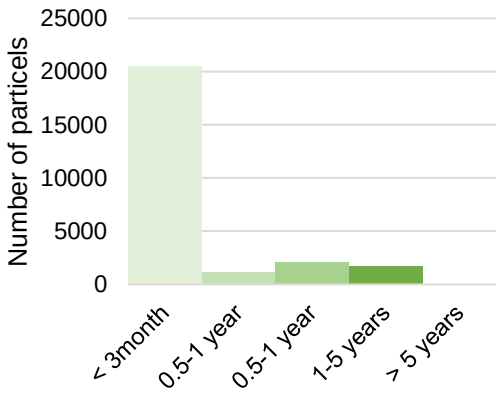

Audrey S — MTT: 1.24 y. Median: 0.00 y

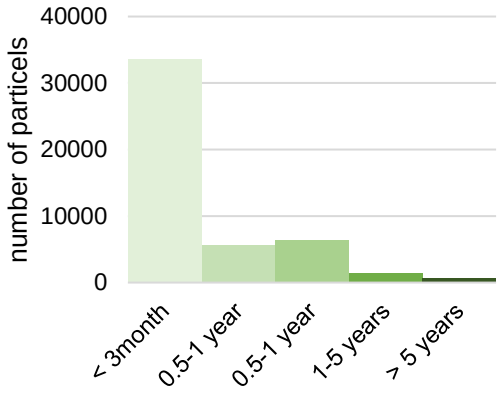

R504 — MTT: 1.33 y. Median: 0.00 y

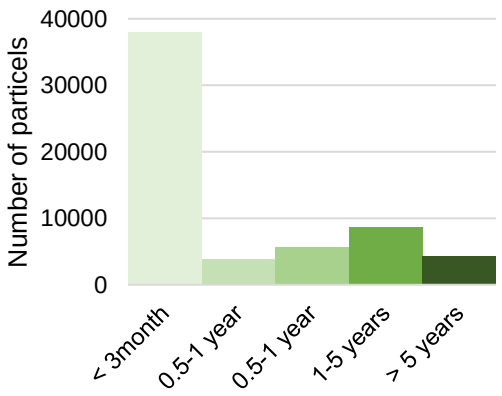

Travel time distribution of particles

Before CFC-12 calibration

SGU2 – MTT: 0.45 y. Median: 0.06 y

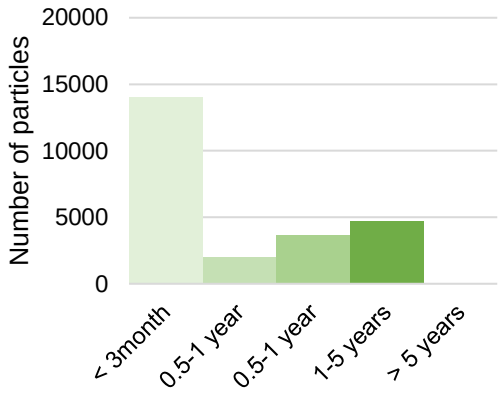

SGU4 – MTT: 16.50 y. Median: 0.09 y

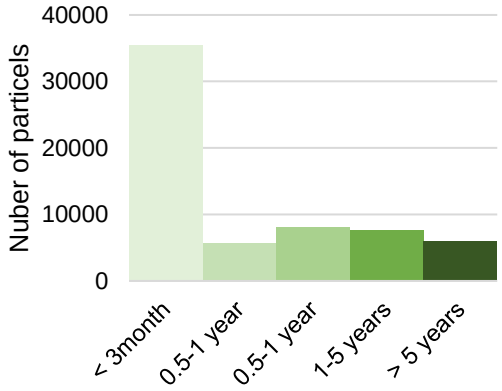

w11 – MTT: 15.09 y. Median: 0.00 y

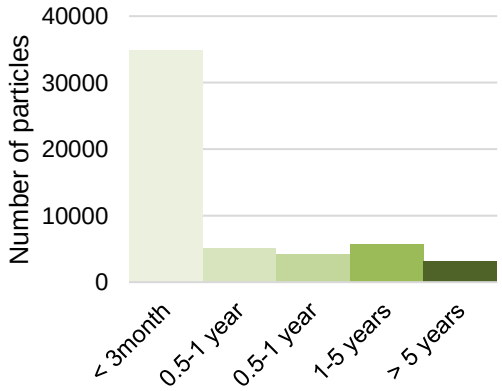

Travel time distribution of particles

After CFC-12 calibration

SGU2 — MTT: 0.40 y. Median: 0.00 y

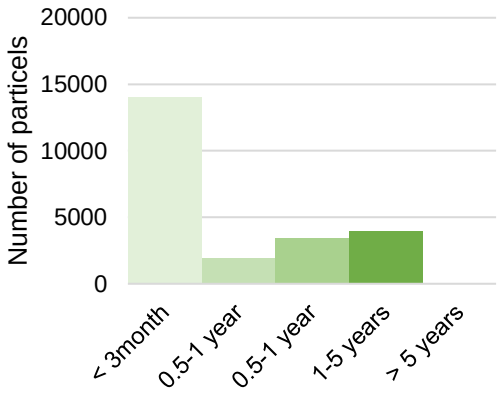

SGU4 — MTT: 10.16 y. Median: 0.14 y

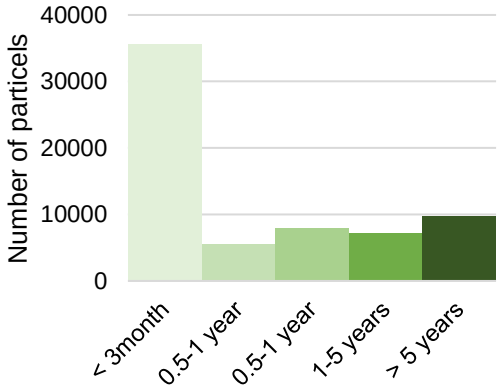

w11 — MTT: 2.74 y. Median: 0.00 y

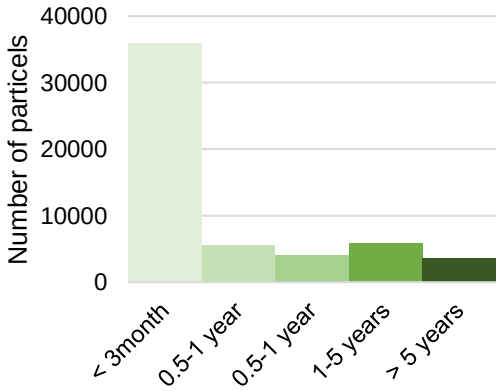

Travel time distribution of particles

Before CFC-12 calibration

w301 – MTT: 2.55 y. Median: 0.00 y

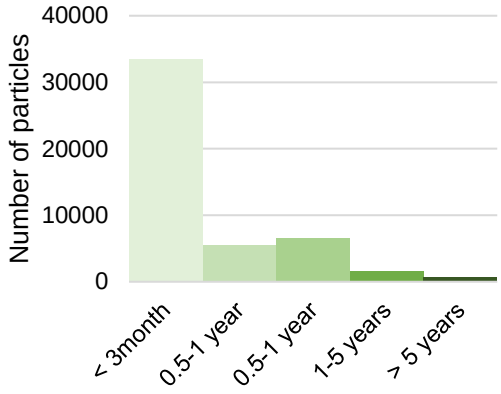

w302 – MTT: 2.55 y. Median: 0.00 y

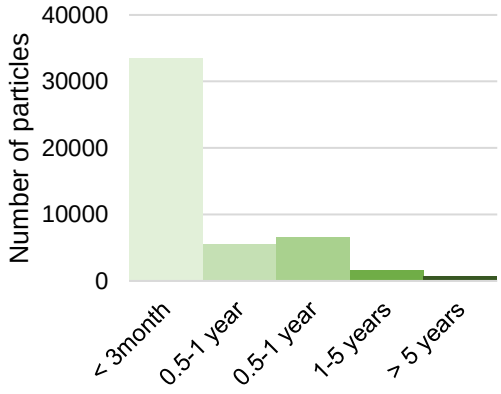

w40 – MTT: 0.42 y. Median: 0.00 y

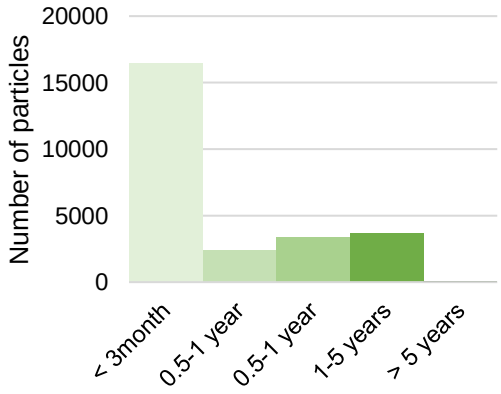

Travel time distribution of particles

After CFC-12 calibration

w301 — MTT: 1.24 y. Median: 0.00 y

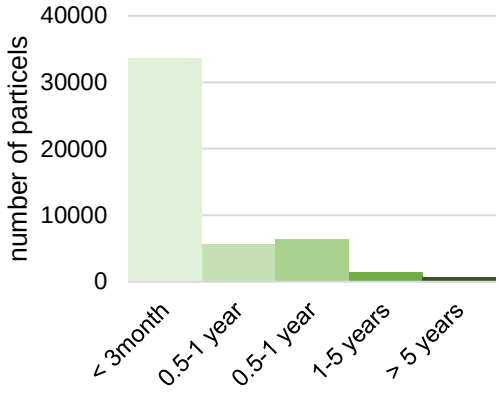

w302 — MTT: 1.24 y. Median: 0.00 y

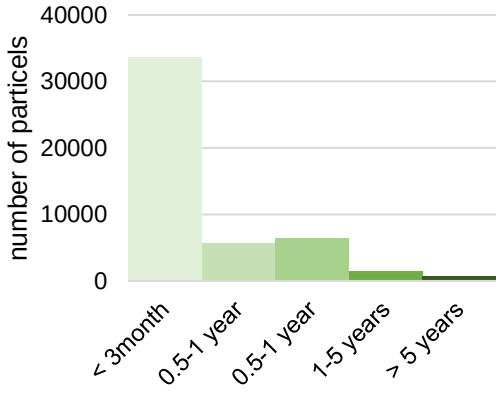

w40 — MTT: 0.82 y. Median: 0.00 y

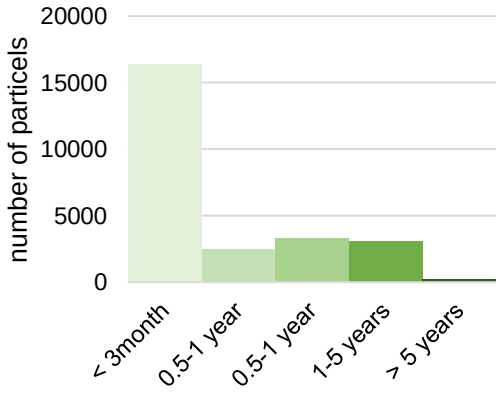

Travel time distribution of particles

Before CFC-12 calibration

w5 – MTT: 35.18 y. Median: 0.03 y

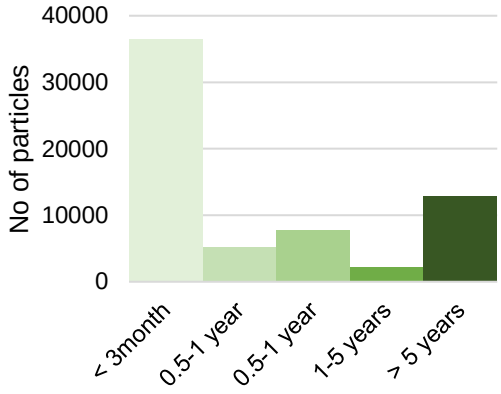

Travel time distribution of particles

After CFC-12 calibration

w5 — MTT: 4.95 y. Median: 0.00 y

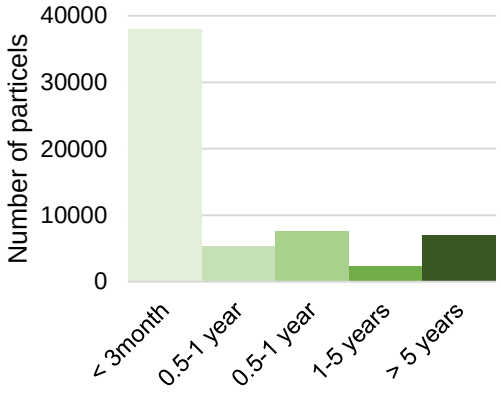

w9 – MTT: 15.09 y. Median: 0.00 y

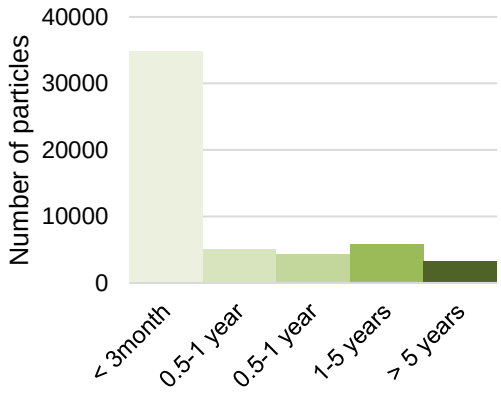

w9 — MTT: 2.74 y. Median: 0.00 y

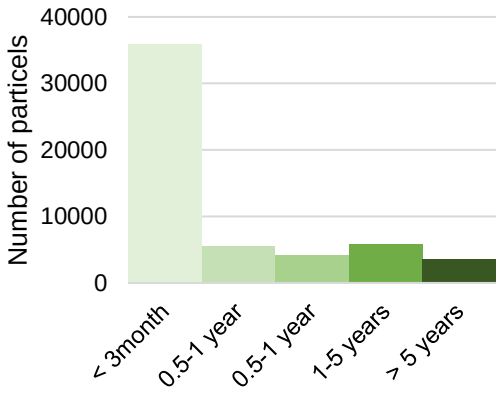

SGU5 – MTT: 0.44 y. Median: 0.00 y

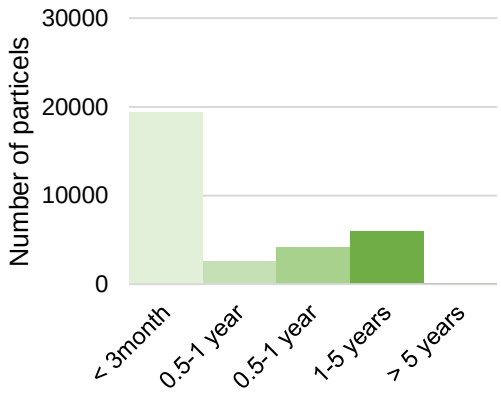

SGU5 — MTT: 0.41 y. Median: 0.00 y

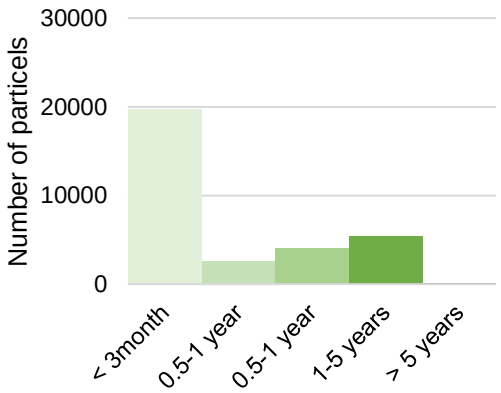

Travel time distribution of particles

Before CFC-12 calibration

w18 – MTT: 21.21 y. Median: 0.12 y

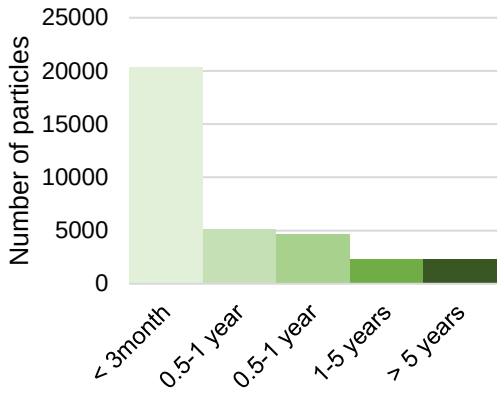

w201 – MTT: 0.28 y. Median: 0.00 y

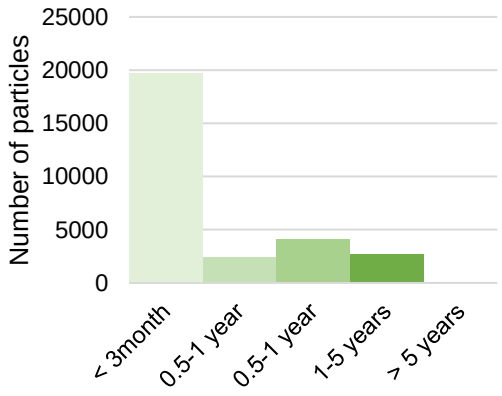

w211 – MTT: 3.19 y. Median: 0.97 y

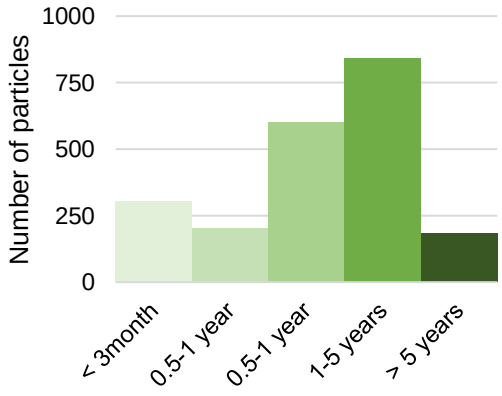

Travel time distribution of particles

After CFC-12 calibration

w18 – MTT: 2.63 y. Median: 0.11 y

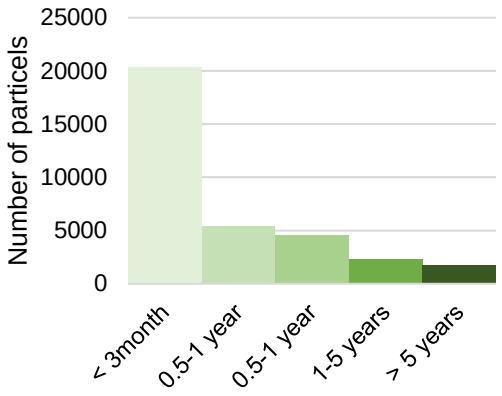

w201 — MTT: 0.27 y. Median: 0.00 y

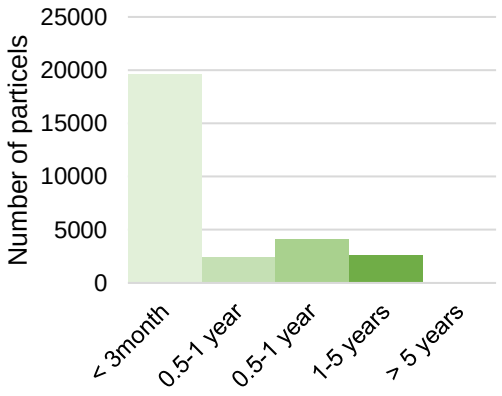

w211 — MTT: 1.82 y. Median: 0.87 y

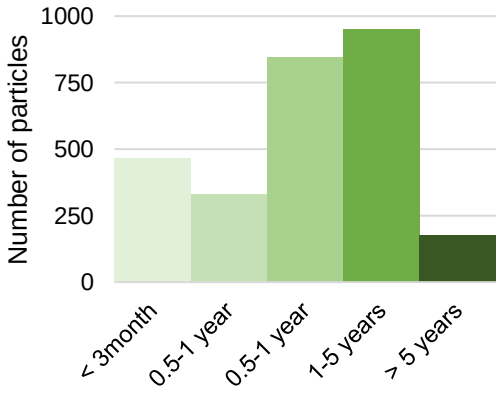

Travel time distribution of particles

Before CFC-12 calibration

w23 – MTT: 0.30 y. Median: 0.00 y

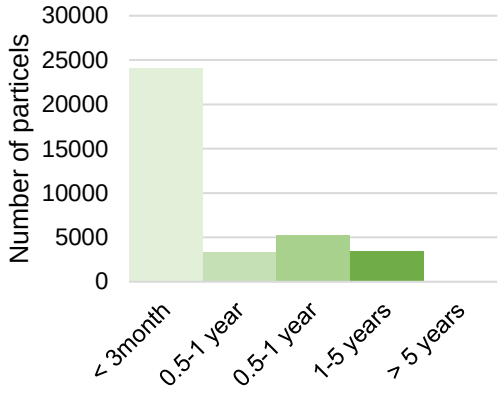

w41 – MTT: 0.28 y. Median: 0.00 y

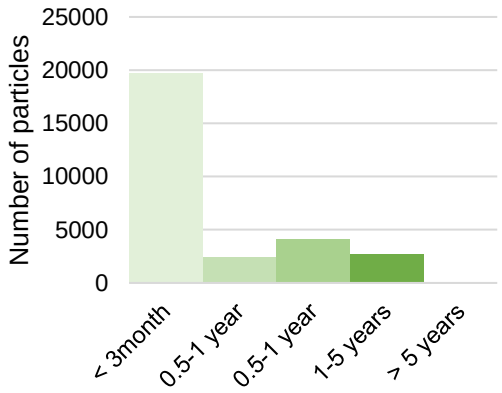

w43– MTT: 5.97 y. Median: 0.74 y

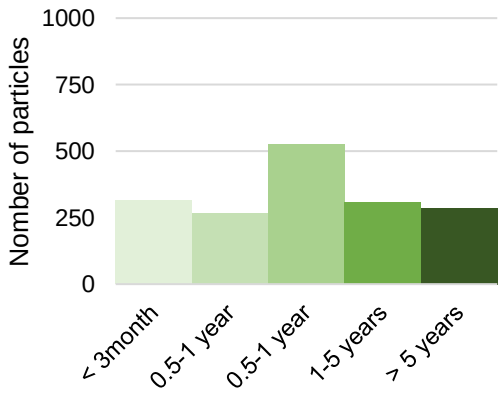

Travel time distribution of particles

After CFC-12 calibration

w23 — MTT: 0.59 y. Median: 0.00 y

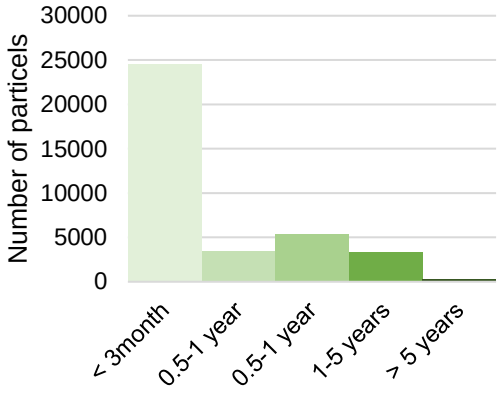

w41 — MTT: 0.27 y. Median: 0.00 y

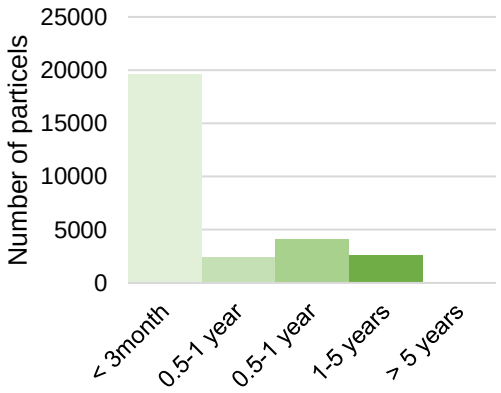

w43 — MTT: 3.27 y. Median: 0.68 y

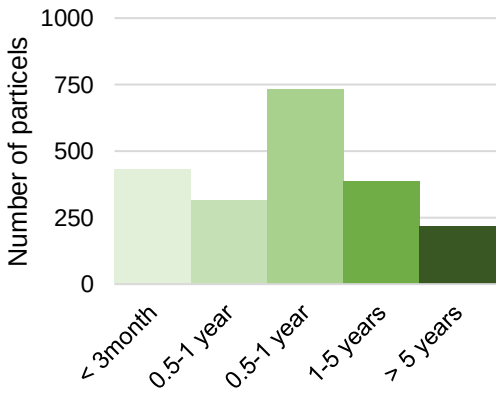

Travel time distribution of particles

Before CFC-12 calibration

w6 – MTT: 192.98 y. Median: 73.86 y

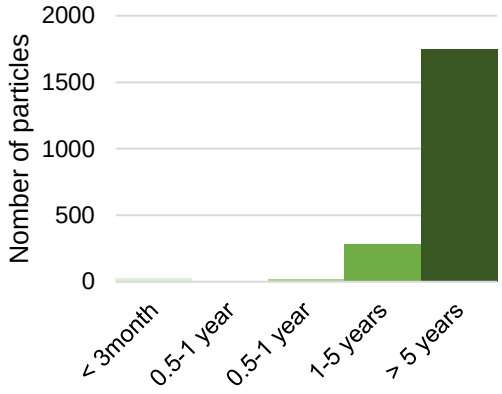

Travel time distribution of particles

After CFC-12 calibration

w6 – MTT: 38.13 y. Median: 24.24 y

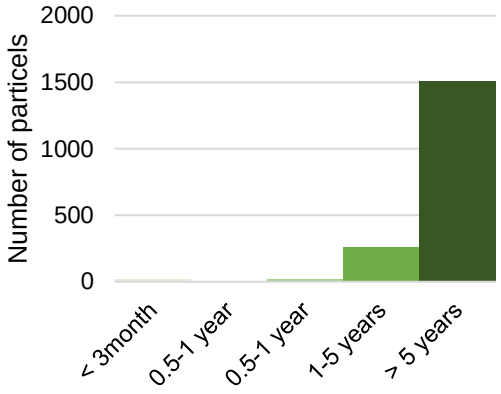

w13 – MTT: 0.00 y. Median: 00.00 y

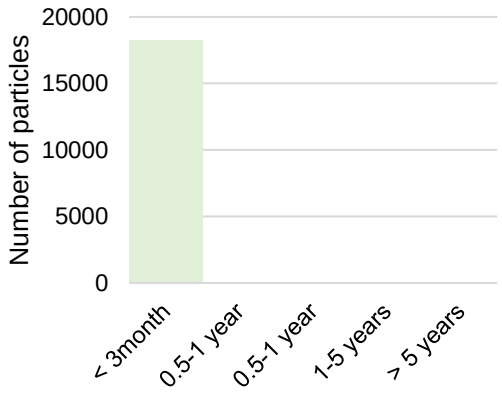

w13 — MTT: 0.01 y. Median: 0.00 y

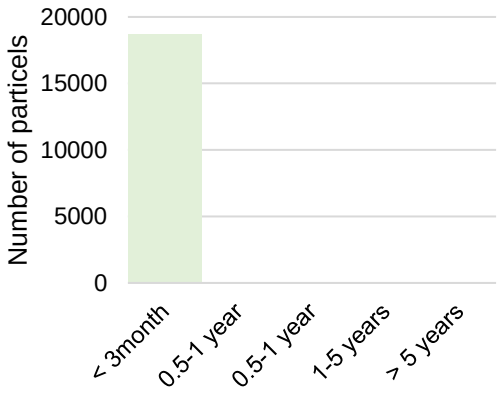

w303 – MTT: 155.82 y. Median: 82.60 y

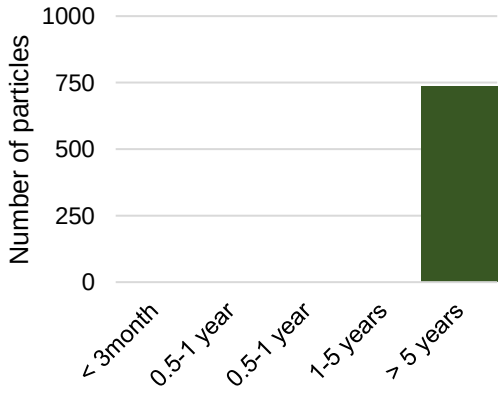

w303 — MTT: 56.17 y. Median: 39.88 y

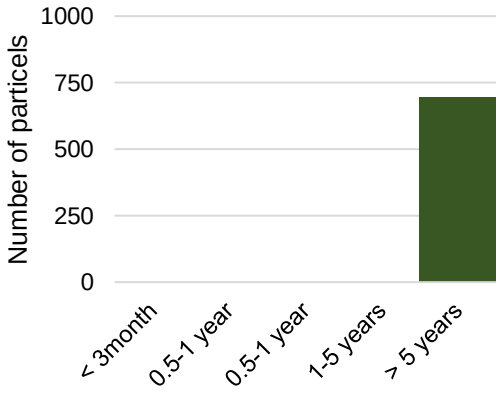

Travel time distribution of particles

Before CFC-12 calibration

w304 – MTT: 325.01 y. Median: 267.10 y

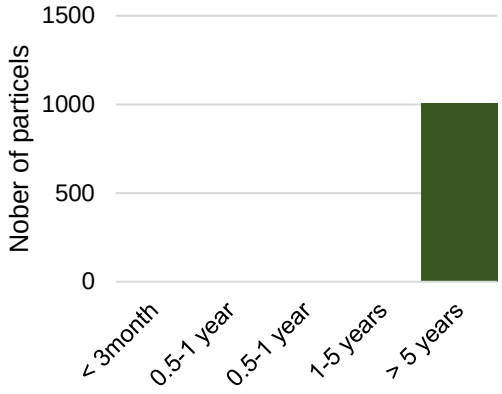

Travel time distribution of particles

After CFC-12 calibration

w304 — MTT: 78.79 y. Median: 73.54 y

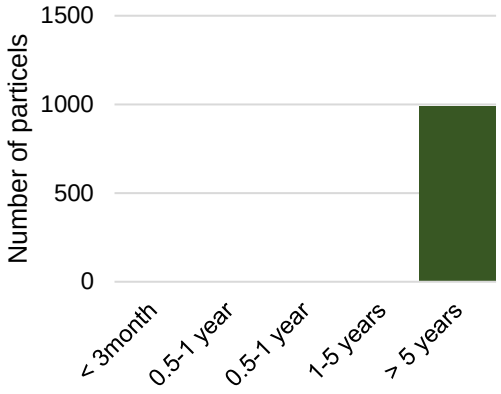

w404 – MTT: 574.25 y. Median: 541.39 y

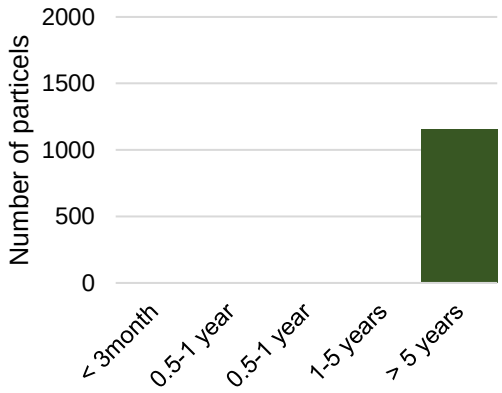

w404 — MTT: 127.91 y. Median: 131.01 y

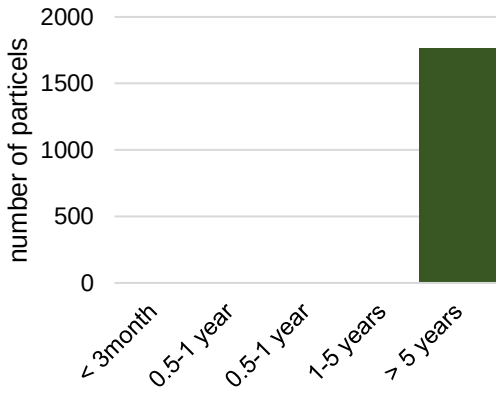

w411 – MTT: 1278.6 y. Median: 1250.5 y

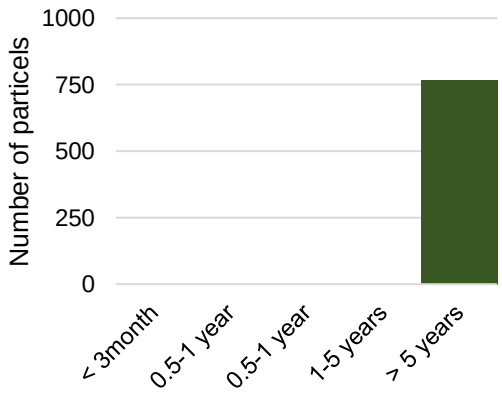

w411 – after CFC calb. MTT: 101.28 y. Median: 97.20 y

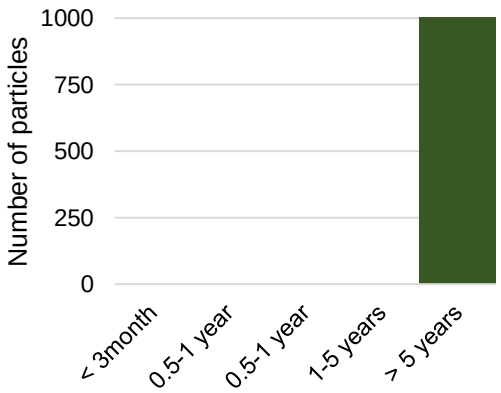

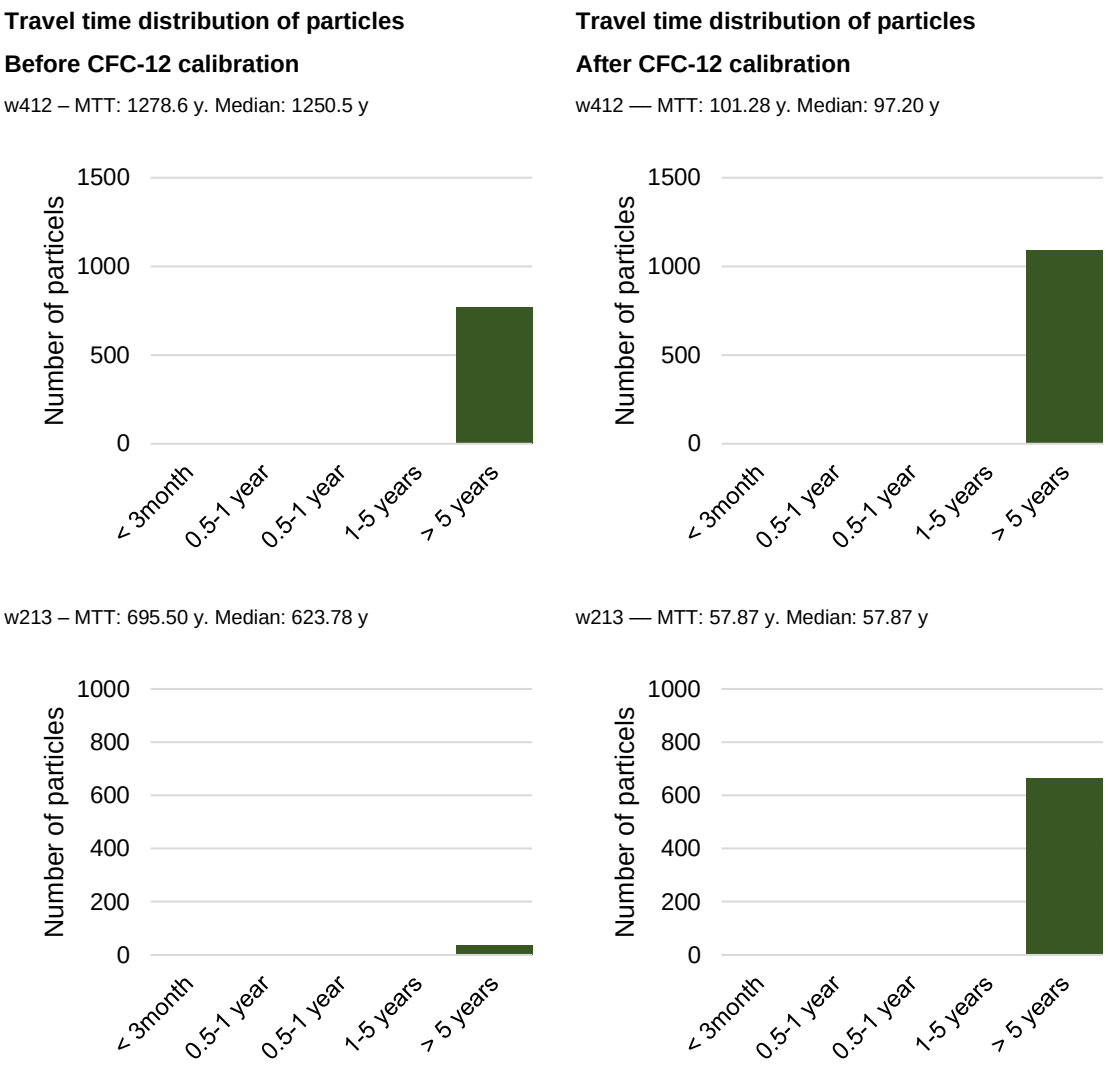

Figure 10-1. *Pre and post-distribution of travel times for wells at different depths, beginning with shallower wells.*